



This discussion paper is/has been under review for the journal Atmospheric Chemistry and Physics (ACP). Please refer to the corresponding final paper in ACP if available.

Radical chemistry at night: comparisons between observed and modelled HO_x, NO₃ and N₂O₅ during the RONOCO project

D. Stone¹, M. J. Evans^{2,3}, H. M. Walker¹, T. Ingham^{1,4}, S. Vaughan¹, B. Ouyang⁵, O. J. Kennedy⁵, M. W. McLeod⁵, R. L. Jones⁵, J. Hopkins^{2,3}, S. Punjabi³, R. Lidster³, J. F. Hamilton^{2,3}, J. D. Lee^{2,3}, A. C. Lewis^{2,3}, L. J. Carpenter^{2,3}, G. Forster⁶, D. E. Oram^{6,7}, C. E. Reeves^{6,7}, S. Bauguitte⁸, W. Morgan^{9,10}, H. Coe^{9,10}, E. Aruffo^{11,12}, C. Dari-Salisburgo¹¹, F. Giammaria¹², P. Di Carlo^{11,12}, and D. E. Heard^{1,4}

¹School of Chemistry, University of Leeds, Leeds, UK

²National Centre for Atmospheric Science, University of York, York, UK

³Department of Chemistry, University of York, York, UK

⁴National Centre for Atmospheric Science, University of Leeds, Leeds, UK

⁵Department of Chemistry, University of Cambridge, Cambridgeshire, UK

⁶School of Environmental Sciences, University of East Anglia, Norwich, UK

⁷National Centre for Atmospheric Science, School of Environmental Sciences, University of East Anglia, Norwich, UK

⁸Facility for Airborne Atmospheric Measurements, Bedfordshire, UK

Title Page

Abstract

Introduction

Conclusions

References

Tables

Figures

◀

▶

◀

▶

Back

Close

Full Screen / Esc

Printer-friendly Version

Interactive Discussion



⁹School of Earth Atmospheric and Environmental Science, University of Manchester, Manchester, UK

¹⁰National Centre for Atmospheric Science, University of Manchester, Manchester, UK

¹¹Center of Excellence CETEMPS Universita' degli studi di L'Aquila, L'Aquila, Italy

¹²Dipartimento di Fisica, Universita' degli studi di L'Aquila, L'Aquila, Italy

Received: 26 March 2013 – Accepted: 29 March 2013 – Published: 11 April 2013

Correspondence to: D. Stone (d.stone@leeds.ac.uk)

Published by Copernicus Publications on behalf of the European Geosciences Union.

Radical chemistry at night

D. Stone et al.

Title Page

Abstract

Introduction

Conclusions

References

Tables

Figures

◀

▶

◀

▶

Back

Close

Full Screen / Esc

Printer-friendly Version

Interactive Discussion



Abstract

The RONOCO aircraft campaign during July 2010 and January 2011 made observations of OH, HO₂, NO₃, N₂O₅ and a number of supporting measurements at night over the UK, and reflects the first simultaneous airborne measurement of these species.

5 We compare the observed concentrations of these short-lived species with those calculated by a box model, constrained by the concentrations of the longer lived species, using a detailed chemical scheme. OH concentrations were below the limit of detection, consistent with the model predictions. The model systematically underpredicts HO₂ by a factor of ~2 and overpredicts NO₃ and N₂O₅ by factors of around 75% and 50%,
10 respectively. Cycling between NO₃ and N₂O₅ is fast and thus we define the NO_{3x} (NO_{3x} = NO₃ + N₂O₅) family. Production of NO_{3x} is overwhelmingly dominated by the reaction of NO₂ with O₃, whereas its loss is dominated by aerosol uptake of N₂O₅, with NO₃ + VOCs and NO₃ + RO₂ playing smaller roles. The production of HO_x and RO_x radicals is mainly due to the reaction of NO₃ with VOCs. The loss of these radicals occurs through a combination of HO₂ + RO₂ reactions, heterogeneous processes and production of HNO₃ from OH + NO₂, with radical propagation primarily achieved
15 through reactions of NO₃ with peroxy radicals. Thus NO₃ at night plays a similar role to both OH and NO during the day in that it both initiates RO_x radical production and acts to propagate the oxidation chain. Model sensitivity to the N₂O₅ aerosol uptake coefficient ($\gamma_{\text{N}_2\text{O}_5}$) is discussed, and we find that a value of $\gamma_{\text{N}_2\text{O}_5} = 0.05$ improves model simulations for NO₃ and N₂O₅, but that these improvements are at the expense of model success for HO₂. Improvements to model simulations for HO₂, NO₃ and N₂O₅
20 can be realised simultaneously on inclusion of additional unsaturated volatile organic compounds, however the nature of these compounds is extremely uncertain.

Radical chemistry at night

D. Stone et al.

Title Page

Abstract

Introduction

Conclusions

References

Tables

Figures

◀

▶

◀

▶

Back

Close

Full Screen / Esc

Printer-friendly Version

Interactive Discussion



1 Introduction

Fundamentally the troposphere acts to oxidise emitted compounds through multiple steps until their volatility or solubility drops sufficiently for them to condense to form aerosol, be removed through contact with the ground or by clouds, or be absorbed by the biosphere or oceans. This oxidation chemistry is of fundamental importance for air quality, climate, food security and ecosystem services. Primary pollutants, such as CH₄, volatile organic compounds (VOCs), oxides of nitrogen and SO₂, are removed by oxidation while secondary pollutants such as O₃ and secondary organic aerosol (SOA) are produced as part of the oxidation chain.

During the day, atmospheric oxidation is initiated by photochemical processes, notably the solar photolysis of O₃ to produce electronically excited oxygen atoms (O(¹D)) that subsequently react with water vapour to produce OH. Over the last few decades there has been extensive research into the processes producing these oxidants and their subsequent chemistry (see for example Stone et al., 2012 and references therein). Much less emphasis has been placed on the nighttime chemistry.

When primary production of OH by solar photolysis cannot occur, other oxidants dominate, notably O₃ and NO₃ (Mihelcic et al., 1993; Carslaw et al., 1997; Salisbury et al., 2001; Fleming et al., 2006; Warneke et al., 2004; Brown et al., 2009, 2011).

Ozone-initiated oxidation of gas phase compounds is primarily limited to alkenes, where ozonolysis of the C=C double bond initiates the oxidation. Ozonolysis has been investigated in a range of laboratory, chamber and field studies (Salisbury et al., 2001; Fleming et al., 2006; Sommariva et al., 2007; Kanaya et al., 1999, 2002, 2007b; Geyer et al., 2003; Malkin et al., 2010; Johnson and Marston, 2008), and has been shown to be responsible for production of OH and HO₂ radicals at night (Salisbury et al., 2001; Fleming et al., 2006; Sommariva et al., 2007; Kanaya et al., 1999, 2002, 2007a; Emmerson and Carslaw, 2009; Ren et al. 2003, 2006; Volkamer et al., 2010).

The nitrate radical (NO₃) is produced by the reaction between O₃ and NO₂. During the day, NO₃ is rapidly photolysed, leading to low daytime concentrations (Wayne

ACPD

13, 9519–9566, 2013

Radical chemistry at night

D. Stone et al.

Title Page

Abstract

Introduction

Conclusions

References

Tables

Figures

◀

▶

◀

▶

Back

Close

Full Screen / Esc

Printer-friendly Version

Interactive Discussion



Radical chemistry at night

D. Stone et al.

Title Page

Abstract

Introduction

Conclusions

References

Tables

Figures

◀

▶

◀

▶

Back

Close

Full Screen / Esc

Printer-friendly Version

Interactive Discussion



et al., 1991; Brown and Stutz, 2012). However, during the night, NO_3 can accumulate, and a rapid equilibrium with N_2O_5 is established through the production of N_2O_5 via $\text{NO}_3 + \text{NO}_2$ followed by rapid thermal decomposition of N_2O_5 back to NO_3 and NO_2 (Wayne et al., 1991; Brown and Stutz, 2012). Losses of N_2O_5 are primarily due to reactions on aerosol surfaces, and there is thus much interest in determination of the aerosol uptake coefficient for N_2O_5 on atmospheric aerosols (Brown et al., 2006, 2009, 2011; Escoreia et al., 2010; Tang et al., 2010; Badger et al., 2006; Thornton and Abbatt, 2005; Hallquist et al., 2003; Thornton et al., 2003; Kane et al., 2001; Hu and Abbatt, 1997; Fried et al., 1994; Van Doren et al., 1991; Hanson and Ravishankara, 1991; Mozurkewich and Calvert, 1998). NO_3 radicals can react with a range of species, including alkenes, aldehydes and RO_x radicals (Wayne et al., 1991; Brown and Stutz, 2012).

Although the initiation of nighttime chemistry by the reactions between NO_3 and O_3 with a range of VOCs is relatively well characterised, the subsequent chemistry has received relatively little attention. Measurements of NO_3 have been overestimated by model calculations in several studies (Mihelcic et al., 1993; Sommariva et al., 2006, 2007), with those of nighttime OH and HO_2 radicals typically underestimated, indicating poor understanding of nighttime tropospheric oxidation processes (Kanaya et al., 1999, 2002, 2007a,b; Emmerson and Carslaw, 2009; Geyer et al., 2003; Faloon et al., 2001; Martinez et al., 2003; Ren et al., 2006).

While a number of nighttime studies at ground-level close to local sources of NO have observed a limited role of NO_3 in nighttime radical production owing to surface losses of NO_3 and the rapid reaction between NO_3 and NO (Salisbury et al., 2001; Fleming et al., 2006; Sommariva et al., 2007; Kanaya et al., 1999, 2002, 2007a,b; Emmerson and Carslaw, 2009; Faloon et al., 2001; Martinez et al., 2003; Ren et al., 2003, 2005, 2006; Volkamer et al., 2010), several studies of NO_3 and N_2O_5 above ground-level and in more remote regions have indicated a more significant role for NO_3 in nighttime radical production and tropospheric oxidation (Platt et al., 1980; Povey et al., 1998; South et al., 1998; Aliwell et al., 1998; Allan et al., 2002; Stutz et al., 2004,

2010; Warneke et al., 2004; Brown et al., 2003, 2004, 2006, 2007, 2009, 2011; Aldener et al., 2006; Sommariva et al., 2009).

5 Measurements of NO_3 and N_2O_5 were made downwind of New York City during the New England Air Quality Study (NEAQS) by cavity ringdown spectroscopy (CRDS) onboard the National Oceanic and Atmospheric Administration (NOAA) research vessel (R/V) *Ronald H. Brown* in summer 2002 (Warneke et al., 2004; Brown et al., 2004; Aldener et al., 2006) and 2004 (Sommariva et al., 2009). While measurements of nighttime composition in New York City led to the conclusion that O_3 -initiated oxidation processes were dominant at night (Ren et al., 2003, 2006), those made during NEAQS indicated little influence of O_3 -initiated VOC oxidation at night, with oxidation of biogenic VOCs dominated by NO_3 (Warneke et al., 2004). Although OH was not measured during NEAQS, the total VOC loss rate owing to reaction with OH over a 24 h period was expected to be $1.7 \times 10^6 \text{ cm}^{-3} \text{ s}^{-1}$, compared to the measured value of $1 \times 10^6 \text{ cm}^{-3} \text{ s}^{-1}$ for NO_3 (Warneke et al., 2004). Conversion of NO_x to HNO_3 at night through NO_3 and N_2O_5 was also found to occur at a comparable rate to that observed during daytime through the $\text{OH} + \text{NO}_2$ reaction, emphasising the importance of nighttime chemistry for determination of NO_x budgets and O_3 production (Warneke et al., 2004; Brown et al., 2004; Aldener et al., 2006).

20 Modelling of NEAQS 2004 shipborne data using the Master Chemical Mechanism (MCM) (<http://mcm.leeds.ac.uk/MCM/home.htm>) (Jenkin et al., 2003; Saunders et al., 2003) demonstrated the importance of peroxy radicals for NO_3 loss, with $\text{NO}_3 + \text{RO}_2$ reactions representing a median of 15% of the total calculated NO_3 gas phase loss, and at times up to 60% of the total NO_3 loss (Sommariva et al., 2006). However, the total sinks for NO_3 and N_2O_5 were still underpredicted, leading to overpredictions of 30 to 50% of observed NO_3 and N_2O_5 concentrations (Sommariva et al., 2006).

25 Aircraft measurements of NO_3 and N_2O_5 at night during NEAQS were significantly higher than the few ppt typically reported at the surface, with the aircraft observations reaching 400 ppt NO_3 and 3.1 ppb N_2O_5 (Brown et al., 2006, 2007, 2009). The high NO_3 concentrations aloft during NEAQS 2004 resulted in significant nighttime oxidation

ACPD

13, 9519–9566, 2013

Radical chemistry at night

D. Stone et al.

Title Page

Abstract

Introduction

Conclusions

References

Tables

Figures

◀

▶

◀

▶

Back

Close

Full Screen / Esc

Printer-friendly Version

Interactive Discussion



Radical chemistry at night

D. Stone et al.

Title Page

Abstract

Introduction

Conclusions

References

Tables

Figures

◀

▶

◀

▶

Back

Close

Full Screen / Esc

Printer-friendly Version

Interactive Discussion



of isoprene, with $\sim 20\%$ of isoprene emissions oxidised at night, and over 90% initiated by NO_3 (Brown et al., 2009). It was suggested that NO_3 -initiated oxidation of isoprene could easily dominate isoprene loss on a regional scale, and it was found that isoprene secondary organic aerosol (SOA) mass derived from NO_3 -oxidation was 50% higher than that from OH-oxidation (Brown et al., 2009). These observations of NO_3 and N_2O_5 loss processes over a wide range of conditions also demonstrated that the uptake coefficient for N_2O_5 ($\gamma_{\text{N}_2\text{O}_5}$) on aerosol particles displays a strong dependence on aerosol composition (Brown et al., 2006). A steady state analysis of NO_3 and N_2O_5 sinks (Brown et al., 2003, 2006), indicated that $\gamma_{\text{N}_2\text{O}_5}$ can vary by over an order of magnitude, largely dependent on the sulfate mass or sulfate to organic ratio of the aerosol (Brown et al., 2006).

High mixing ratios of NO_3 and N_2O_5 (up to 400 ppt and 2 ppb, respectively) were also reported in a subsequent aircraft study using the NOAA P-3 aircraft during the Texas Air Quality Study (TexAQS) in 2006 (Brown et al., 2011). Budget analyses for the campaign indicated that VOC oxidation at night was rapid, with the total rate of NO_3 -initiated oxidation typically 3 to 5 times that initiated by O_3 , and NO_3 reactivity indicating the presence of unmeasured plumes of highly reactive VOCs (Brown et al., 2011). Loss of NO_3 was dominated by its chemistry with unsaturated VOCs, with only 14 to 28% of NO_3 loss occurring indirectly through heterogeneous chemistry of N_2O_5 , although significant uncertainties in the N_2O_5 aerosol uptake coefficient were noted (Brown et al., 2011). Reactions of NO_3 with peroxy radicals were estimated as contributing between 1 and 4% of the total NO_3 loss, although no direct measurements of RO_2 were available, with measurements of PAN used to estimate RO_2 concentrations as being equal to the acetylperoxy ($\text{CH}_3\text{C}(\text{O})\text{O}_2$) radical concentration produced by thermal decomposition of PAN (Brown et al., 2011).

Previous studies have shown that nighttime chemistry plays a significant role in defining the chemistry of the troposphere. However, there are significant uncertainties in the chemistry of the atmosphere at night. Many of these uncertainties are due to the lack of simultaneous observations of OH, HO_2 , NO_3 and N_2O_5 . Those observations

that do exist often occur within the centres of cities where NO emissions are high, with NO₃ concentrations thus kept low. These “inner city” conditions are not representative of most of the planet and thus do not offer suitable conditions for an evaluation of our understanding of nighttime chemistry.

In this paper we take advantage of simultaneous aircraft measurements of OH, HO₂, NO₃ and N₂O₅, together with the concentrations of long lived components made away from recent emissions to analyse our understanding of nighttime chemistry as manifested by a constrained box model. We provide a brief overview of the campaign in Sect. 2 and measurement techniques in Sect. 3, followed by a description of the model approach in Sect. 4. In Sect. 5 we describe comparisons between modelled and observed concentrations and in Sect. 6 examine the processes controlling atmospheric composition at night. Potential sources of model uncertainty are discussed in Sect. 7, with suggestions for future work in Sect. 8 and conclusions drawn in Sect. 9.

2 The RONOCO campaign

The ROle of Nighttime chemistry in controlling the Oxidising Capacity of the Atmosphere (RONOCO) project took place in July 2010 and January 2011. Aircraft measurements were made at altitudes up to 6400 m over the UK and the North Sea onboard the UK FAAM BAe146 aircraft, based at East Midlands Airport (52.8° N, 1.3° W) during the campaign. The main objectives of the RONOCO campaign were to obtain comprehensive measurements of nighttime composition to further our understanding of nighttime chemistry thus enabling quantification of the key processes controlling atmospheric chemistry at night, and ultimately to facilitate assessment of the regional and global impacts of nighttime chemistry on air quality and climate change.

Measurements of HO_x were made on 16 flights throughout the campaign (7 flights in July 2010 and 9 flights in January 2011), while measurements of NO₃ and N₂O₅ were made on 17 flights (9 flights in July 2010 and 8 flights in January 2011). In our analysis we combine all of these flights into a single dataset. Figure 1 shows the locations of

Title Page

Abstract

Introduction

Conclusions

References

Tables

Figures

◀

▶

◀

▶

Back

Close

Full Screen / Esc

Printer-friendly Version

Interactive Discussion



HO_x, NO₃ and N₂O₅ measurements made during RONOCO. We focus here on the analysis of measurements made at night, defined as periods when the solar zenith angle was greater than 99°, and thus do not include data from flights made in daylight hours or during dawn or dusk periods. Data from flight B537 (20 July 2010) has also been excluded from our analysis owing to a number of atypical observations during this flight which are discussed elsewhere (Kennedy et al., 2011; Walker et al., 2013).

3 Measurements during RONOCO

3.1 Detection of OH and HO₂

OH and HO₂ radicals were measured by laser-induced fluorescence (LIF) spectroscopy at low pressure using the Fluorescence Assay by Gas Expansion (FAGE) technique (Heard and Pilling, 2003). The instrument has been described in detail elsewhere (Commane et al., 2010; Stone et al., 2011), and only a brief description is given here.

Ambient air from the aircraft exterior is drawn into a fluorescence cell maintained at pressures ranging from 1.9 Torr at sea level to 1.2 Torr at 6 km. The fluorescence cell has two excitation axes, with excess NO added at the second axis to titrate HO₂ to OH, enabling simultaneous detection of OH and HO₂. OH radicals in both excitation axes are excited by laser light at $\lambda \sim 308$ nm, generated by a solid state Nd:YAG pumped Ti:Sapphire laser system which is frequency tripled (Bloss et al., 2003). Channel photomultiplier tubes coupled to gated photon counters were used to detect the $A^2\Sigma^+ - X^2\Pi$; OH fluorescence signal at $\lambda \sim 308$ nm.

Calibration of the instrument is achieved by measurement of the fluorescence signal from known concentrations of OH and HO₂, produced by the photolysis of water vapour, and was performed over a range of conditions before and after the RONOCO campaign. The instrument sensitivity to OH (C_{OH}) was determined to be $(2.50 \pm 0.1) \times 10^{-8} \text{ s}^{-1} \text{ cm}^3 \text{ mW}^{-1}$ and that to HO₂ (C_{HO_2}) was determined to be

[Title Page](#)[Abstract](#)[Introduction](#)[Conclusions](#)[References](#)[Tables](#)[Figures](#)[◀](#)[▶](#)[◀](#)[▶](#)[Back](#)[Close](#)[Full Screen / Esc](#)[Printer-friendly Version](#)[Interactive Discussion](#)

measured in a separate cavity maintained at 80 °C following its thermal dissociation to NO₃ and NO₂ at 120 °C in a heater situated prior to the cavity entrance, and thus measured as the sum of ambient NO₃ and thermally dissociated N₂O₅. The third cavity enables detection of NO₂ using light provided by a blue LED with output centred around 460 nm.

A crystalline source of N₂O₅, stabilised at temperatures between -80 and -77 °C, was used to provide known amounts of NO₃ and N₂O₅ to facilitate calibration of the instrument in the laboratory. The in-flight 1σ LOD (determined at a pressure of 0.7 bar) for NO₃ was found to be 1.1 ppt for a 1 s integration time, with a corresponding LOD of 2.4 ppt for NO₃ + N₂O₅.

3.3 Supporting measurements

Measurements from several other instruments onboard the BAe146 during the RONOCO campaign have been used in the analysis presented here. Details of these supporting measurements are summarised in Table 1.

4 Model approach

Observations of OH, HO₂, NO₃ and N₂O₅ have been interpreted using the Dynamically Simple Model of Atmospheric Chemical Complexity (DSMACC), which is described in detail by Emmerson and Evans (2009) and Stone et al. (2010). DSMACC is a zero-dimensional model using the Kinetic Pre-Processor (KPP) (Sandu and Sander, 2006), and in this work uses a chemistry scheme described by the Master Chemical Mechanism version 3.2 (MCM v3.2 <http://mcm.leeds.ac.uk/MCM/home.htm>) (Jenkin et al., 2003; Saunders et al., 2003). The MCM contains near explicit degradation schemes for 143 primary species, resulting in 6700 species in approximately 17 000 reactions and representing the most detailed and comprehensive chemistry scheme available for modelling tropospheric composition. Simulations reported here use degradation

Title Page

Abstract

Introduction

Conclusions

References

Tables

Figures

◀

▶

◀

▶

Back

Close

Full Screen / Esc

Printer-friendly Version

Interactive Discussion



chemistry for ethane, propane, *iso*-butane, *n*-butane, *iso*-pentane, *n*-pentane, sum of 2 + 3-methylpentane, *n*-hexane, *n*-heptane, *n*-octane, ethene, propene, acetylene, *trans*-2-butene, 1-butene, *cis*-2-butene, *iso*-butene, 1,3-butadiene, *trans*-2-pentene, 1-pentene, isoprene, benzene, toluene, ethylbenzene, xylene, methacrolein and acetone.

5 The scheme used contains ~ 2000 species in ~ 8000 reactions.

Heterogeneous loss of several species (OH, HO₂, CH₃O₂, NO₃, N₂O₅ and HNO₃) to aerosol surfaces was represented in the model by parameterisation of a first-order loss process to the aerosol surface (Ravishankara, 1997):

$$k' = c_g A \gamma_x / 4 \quad (1)$$

$$10 \quad c_g = (8RT / \pi M_w)^{1/2} \quad (2)$$

where k' is the first-order rate coefficient for heterogeneous loss, c_g is the mean molecular speed of the gas (Eq. 1), A is the aerosol surface area per unit volume and γ_x is the uptake coefficient for species X , R is the universal gas constant, T is the temperature and M_w is the molecular weight of the gas. For HO₂, $\gamma_{\text{HO}_2} = 0.028$ is used, based on the mean value reported by the parameterisation by Macintyre and Evans (2011). For N₂O₅, $\gamma_{\text{N}_2\text{O}_5} = 0.020$ is used, based on the mean value reported from the parameterisation by Evans and Jacob (2005). Sensitivity to aerosol uptake coefficients is discussed in Sect. 7.2.

20 An additional first-order loss process for each species in the model is also included to represent deposition processes, with the first-order rate set to be equivalent to a lifetime of approximately 24 h. Model sensitivity to this parameter is discussed in Sect. 7.1.

All aircraft measurements are merged onto a 60 s timebase. Time points with observations of OH or HO₂ are modelled if observations of physical state (latitude, longitude, pressure, temperature and water vapour concentration), aerosol surface area and concentrations of CO, O₃, NO₂, NO₃ and VOCs are available. A summary of concentrations used to constrain the model is given in Table 2. Observed concentrations of CO, O₃, H₂O, VOCs and aerosol surface area for each 60 s time point are fixed and held constant throughout the corresponding model run, with concentrations

Title Page

Abstract

Introduction

Conclusions

References

Tables

Figures

◀

▶

◀

▶

Back

Close

Full Screen / Esc

Printer-friendly Version

Interactive Discussion



of CH₄ and H₂ kept constant at values of 1770 ppb (NOAA CMDL flask analysis, ftp://ftp.cmdl.noaa.gov/ccg/ch4/) and 550 ppb (Ehhalt and Rohrer, 2009; Novelli et al., 1999) respectively. Species which were not observed are set initially to zero in the model.

Constraints on nitrogen oxides (NO, NO₂, NO₃, N₂O₅, HONO and HO₂NO₂) were applied using the method described by Stone et al. (2010), with the primary constraint placed on NO₂. Thus, the initial concentration of NO₂ in the model is set to its observed value and the concentrations of each nitrogen oxide species, including NO₂, is permitted to vary according to its photochemistry as the model runs forwards. At the end of each 24 h period in the model, the calculated concentration of NO₂ is compared to its observed concentration, and the concentrations of all nitrogen oxide species are fractionally increased or decreased such that the modelled and observed concentrations of NO₂ are the same. The model is integrated forwards in time with diurnally varying photolysis rates until a diurnal steady state is reached, typically requiring between 5 and 10 days. Thus at the point of comparison between the model and observations we have a modelled NO₂ concentration equal to the observed concentration, together with concentrations of the other NO_x species (NO, NO₃, N₂O₅, HONO, HO₂NO₂) consistent with that NO₂ concentration, the concentration of the other measured species, and the time since darkness fell.

Following the work of Fuchs et al. (2011), model calculations described in this work include representation of potential RO₂ interferences in LIF measurements of HO₂. We thus describe observed to modelled comparisons of HO₂^{*}, where HO₂^{*} = HO₂ + *f*RO₂, with the factor *f* derived from a combination of experimental parameters and MCM chemistry, as described in the appendix. For the RONOCO campaign, potential interferences in HO₂ measurements are expected to be small on average, with HO₂^{*} = [1.15 × HO₂] + 2 × 10⁵ cm⁻³.

[Title Page](#)[Abstract](#)[Introduction](#)[Conclusions](#)[References](#)[Tables](#)[Figures](#)[◀](#)[▶](#)[◀](#)[▶](#)[Back](#)[Close](#)[Full Screen / Esc](#)[Printer-friendly Version](#)[Interactive Discussion](#)

5 Model performance

Figure 2 shows the model performance for HO_2^* , NO_3 and N_2O_5 . Modelled concentrations of OH were on the order of 10^4 cm^{-3} (mean $(2.43 \pm 2.32) \times 10^4 \text{ cm}^{-3}$; median = $1.69 \times 10^4 \text{ cm}^{-3}$) and were consistently below the 1σ instrumental limits of detection of $1.8 \times 10^6 \text{ cm}^{-3}$ in summer and $6.4 \times 10^5 \text{ cm}^{-3}$ in winter (for 5 min averaging periods). We do not consider the model performance for OH in any more detail.

The model displays a tendency to underpredict HO_2^* and overpredict NO_3 and N_2O_5 , as shown in Fig. 2. For HO_2^* , the line of best fit is given by $[\text{HO}_2^*]_{\text{mod}} = \{0.45 \times [\text{HO}_2^*]_{\text{obs}}\} + 2.95 \times 10^6 \text{ cm}^{-3}$, with that for NO_3 given by $[\text{NO}_3]_{\text{mod}} = \{1.75 \times [\text{NO}_3]_{\text{obs}}\} - 2.33 \text{ ppt}$ and the best fit line for N_2O_5 described by $[\text{N}_2\text{O}_5]_{\text{mod}} = \{1.46 \times [\text{N}_2\text{O}_5]_{\text{mod}}\} - 42.43 \text{ ppt}$.

Model underpredictions for nighttime HO_2 of a similar magnitude have been observed in a number of previous studies, and, where observations are available, model underpredictions of HO_2 tend to coincide with underpredictions of RO_2 and overpredictions of NO_3 . Measurements of peroxy radicals in the Black Forest, Germany, were underestimated by a factor of 3 to 4, coinciding with an overprediction of NO_3 by a factor of ~ 2 , with discrepancies for both NO_3 and peroxy radicals reconciled by consideration of the impact of unmeasured monoterpenes (Mihelcic et al., 1993). Observations of HO_2 at night on Rishiri Island, Japan, were strongly correlated with monoterpene emissions (Kanaya et al., 2002, 2007a) and were also generally underestimated by model calculations (Kanaya et al., 1999; 2002, 2007a). Model calculations for the Southern Oxidant Study (SOS) in Nashville, USA, underpredicted nighttime observations of HO_2 by a factor of 2 to 8, partly owing to the limited $\text{NO}_3 + \text{VOC}$ and $\text{NO}_3 + \text{RO}_2$ chemistry in the model (Martinez et al., 2003). Model underpredictions for nighttime HO_2 have also been reported for campaigns near London (Emmerson and Carslaw, 2009), in New York (Ren et al., 2003, 2006) and Tokyo (Kanaya et al., 2007a), with investigation of the model discrepancy for the Tokyo campaign indicating the presence of unmeasured VOCs which, if included in the model, could reconcile the modelled HO_2

[Title Page](#)[Abstract](#)[Introduction](#)[Conclusions](#)[References](#)[Tables](#)[Figures](#)[◀](#)[▶](#)[◀](#)[▶](#)[Back](#)[Close](#)[Full Screen / Esc](#)[Printer-friendly Version](#)[Interactive Discussion](#)

with the observations (Kanaya et al., 2007). The presence of unmeasured VOCs was also thought to be responsible for discrepancies between observed concentrations of NO_3 and calculations of NO_3 reactivity from measured sources and sinks during the TexAQS campaign (Brown et al., 2011).

In order to show the important processes occurring within the model and to thus provide insights into improving model fidelity we now diagnose the chemical processes occurring within the model. We start our analysis with the budgets of NO_3 and N_2O_5 , we then turn our attention to the wider RO_x family and finally to HO_x , HO_2 and OH .

6 Budget analyses

6.1 NO_3 and N_2O_5 budgets

NO_3 and N_2O_5 rapidly interconvert, with reaction of NO_3 with NO_2 and thermal decomposition of N_2O_5 occurring at a faster rate ($\sim 3 \times 10^7 \text{ cm}^{-3} \text{ s}^{-1}$) than the conversion between OH and HO_2 ($\sim 3 \times 10^4 \text{ cm}^{-3} \text{ s}^{-1}$ during RONOCO). This leads us to define the NO_{3x} family, where $\text{NO}_{3x} = \text{NO}_3 + \text{N}_2\text{O}_5$. Production of NO_{3x} occurs almost exclusively through the production of NO_3 by $\text{O}_3 + \text{NO}_2$, with minor production channels ($< 0.01\%$) including $\text{OH} + \text{HNO}_3$ and reactions of Criegee biradicals with NO_2 .

Figure 3 shows the loss pathways for NO_{3x} at night, displayed as the probability distribution functions for the percentage contribution of each process to the total NO_{3x} loss. The largest loss of NO_{3x} is typically due to heterogeneous processes, through the uptake and hydrolysis of N_2O_5 on aerosol surfaces, representing 64 % of the total NO_{3x} loss averaged over all simulated data points. However, there is high variability in the fraction of the total loss through heterogeneous processes, as displayed in Fig. 3. Reactions of NO_3 with VOCs comprises 10 % of the total NO_{3x} loss on average, with a maximum value of 40 % when VOC concentrations are high and aerosol loadings low. Loss of NO_{3x} through reactions of NO_3 with peroxy radicals represents 19 % of the total (11 % from organic RO_2 and 8 % from HO_2) on average, but there are data points

[Title Page](#)[Abstract](#)[Introduction](#)[Conclusions](#)[References](#)[Tables](#)[Figures](#)[◀](#)[▶](#)[◀](#)[▶](#)[Back](#)[Close](#)[Full Screen / Esc](#)[Printer-friendly Version](#)[Interactive Discussion](#)

where the loss of NO_{3x} through such reactions reaches 71 %. Thus, although in a mean sense the loss of NO_{3x} from the atmosphere is dominated by the heterogeneous uptake of N_2O_5 onto aerosol, there are significant other processes which can dominate under certain conditions.

These results are consistent with previous studies. Modelling of the NEAQS 2004 shipborne campaign using the MCM revealed similar losses of NO_3 to RO_2 in the marine boundary layer to those presented here, with a mean contribution of 19 % to the total gas phase NO_3 loss and a maximum of up to 60 % (Sommariva et al., 2009). In contrast, analysis of NO_3 budgets for the airborne TexAQS 2006 campaign suggested that only 1 to 4 % of the total NO_{3x} loss occurred as a result of reactions of NO_3 with peroxy radicals (Brown et al., 2011). However, no peroxy radical measurements were made during TexAQS, and RO_2 concentrations were estimated using observations of PAN and its thermal decomposition rate, and were thus almost certainly a significant underestimate, as noted in the analysis (Brown et al., 2011). Model calculations in this work indicate that the peroxy radical derived from thermal decomposition of PAN represents a maximum of 15 % of the total organic peroxy radical concentration during RONOCO, with a median value of 0.3 %.

6.2 RO_x radical budgets

RO_x radicals ($\text{RO}_2 + \text{RO} + \text{HO}_2 + \text{OH}$) play a central role in the chemistry of the troposphere. Figure 4 shows the production and loss processes for RO_x radicals at night during RONOCO (note that the discussion in this section concerns HO_2 and not HO_2^*). Initiation of radicals at night, and thus of nighttime oxidation chemistry, is dominated by reactions of NO_3 with unsaturated VOCs, with a mean campaign contribution of 80 % compared to 18 % for radical production by alkene ozonolysis reactions. Figure 5 shows that of the VOCs measured during the campaign (Table 2), the dominant species in terms of NO_3 reactivity are *iso*-butene (36 %), *trans*-2-butene (27 %) and, during the summer campaign, isoprene (10 %), with O_3 reacting mainly with *trans*-2-butene (51 %), propene (22 %), ethene (13 %) and *iso*-butene (5 %). Reactions of NO_3 with

[Title Page](#)[Abstract](#)[Introduction](#)[Conclusions](#)[References](#)[Tables](#)[Figures](#)[◀](#)[▶](#)[◀](#)[▶](#)[Back](#)[Close](#)[Full Screen / Esc](#)[Printer-friendly Version](#)[Interactive Discussion](#)

aldehydes also result in radical production at night, with $\text{NO}_3 + \text{HCHO}$ contributing the greatest influence from aldehyde species.

Figure 4 shows that radical loss is controlled by a number of processes. Production of peroxides, through $\text{RO}_2 + \text{HO}_2$ and $\text{HO}_2 + \text{HO}_2$, represents 21 % of the RO_x radical loss, followed by production of HNO_3 by $\text{OH} + \text{NO}_2$ (16 %), decomposition reactions of RO radicals to produce stable products (14 %) and heterogeneous losses (2 %). The large fraction of remaining loss processes (47 % of the total) is comprised largely of a myriad of RONO_2 and RO_2NO_2 production routes.

Overall, reactions of NO_3 with VOCs typically control the production of radicals during the campaign, with the unsaturated C_4 compounds dominating. There are a significant number of radical loss processes which produce organic nitrogen compounds, peroxides and nitric acid.

6.3 HO_x radical budgets

The processes controlling production and loss of nighttime HO_x ($\text{HO}_x = \text{OH} + \text{HO}_2$) radicals during RONOCO are shown in Fig. 6. Alkoxy radicals (RO), produced primarily following production of RO_2 from $\text{NO}_3 + \text{alkene}$ reactions and the subsequent reactions of RO_2 with NO_3 , are a major source of HO_x , producing HO_2 through $\text{RO} + \text{O}_2$ reactions and on average representing 63 % of the total HO_x production. Specifically, the reaction of methoxy radicals (CH_3O) with O_2 dominates the HO_x production from RO radicals (31 % of the total HO_x production), with CH_3O primarily produced at night by $\text{CH}_3\text{O}_2 + \text{NO}_3$, and nighttime CH_3O_2 production primarily occurring through OH-initiated oxidation of CH_4 (48 %) and alkene ozonolysis reactions (37 %). Alkene ozonolysis reactions also produce OH and HO_2 radicals directly through the decomposition of Criegee intermediates, and are responsible for 20 % of the total HO_x production. A further 17 % of HO_x radicals are generated as a result of direct HO_2 production by $\text{NO}_3 + \text{HCHO}$, using model calculated HCHO concentrations.

Reactions of HO_2 producing peroxides ($\text{HO}_2 + \text{RO}_2$ and $\text{HO}_2 + \text{HO}_2$) and formation of HNO_3 by the reaction of OH with NO_2 represent major sinks for HO_x radicals,

Title Page

Abstract

Introduction

Conclusions

References

Tables

Figures

◀

▶

◀

▶

Back

Close

Full Screen / Esc

Printer-friendly Version

Interactive Discussion



comprising 23% and 25% of the total loss, respectively. Heterogeneous loss of OH and HO₂, primarily through aerosol uptake of HO₂, represents 11% of the total HO_x sink, with the remainder occurring primarily through reactions of OH with VOCs, and OH + CH₄ alone constituting 19% of the total HO_x sink.

Figure 7 shows the processes controlling modelled nighttime HO₂ concentrations during the campaign. Production of HO₂ is dominated by RO + O₂ reactions, comprising 42% of the total on inclusion of CH₃O + O₂. Despite the low OH concentrations at night, there is also significant HO₂ production via OH + CO (31%). Alkene ozonolysis reactions represent 5% of the total HO₂ production, on average, with reactions of HCHO with NO₃ and OH contributing 8% and 6% to the total HO₂ production, respectively.

The dominant loss pathways for HO₂ are through reaction with NO₃ (45% of the total) and O₃ (27%), with both reactions representing radical propagation routes. Reactions of HO₂ with other peroxy radicals (both HO₂ and RO₂) constitute 17% of the HO₂ loss, while uptake onto aerosols contributes only 7% to the total HO₂ loss.

Production of OH at night occurred primarily through the reactions of HO₂ with NO₃ (53%) and O₃ (33%), with OH loss processes dominated by its reactions with CO (35%), NO₂ (21%) and CH₄ (12%).

6.4 Summary of budget analyses

Figure 8 shows a summary of the processes controlling nighttime composition during RONOCO. In general we see a significant coupling between the NO_{3x} and RO_x families. The NO_{3x} family is primarily controlled by the balance between its production from the reaction of NO₂ and O₃ and its loss predominantly to aerosols through N₂O₅. However, the component of the loss not through this path (36%, on average) is responsible for a dynamic organic chemistry. The reactions of NO₃ with alkenes, and of NO₃ with C₄-alkenes in particular, represent the dominant radical source at night during RONOCO, with radical losses owing to a combination of heterogeneous processes, peroxide formation (through HO₂ + RO₂ and HO₂ + HO₂), decomposition of alkoxy radicals and

[Title Page](#)[Abstract](#)[Introduction](#)[Conclusions](#)[References](#)[Tables](#)[Figures](#)[◀](#)[▶](#)[◀](#)[▶](#)[Back](#)[Close](#)[Full Screen / Esc](#)[Printer-friendly Version](#)[Interactive Discussion](#)

formation of HNO_3 through the reaction of OH with NO_2 . The propagation of the radical oxidation chemistry, which during the day would be controlled by NO, is at night controlled by NO_3 . Thus the NO_3 radical acts both as a chain initiator (like OH during the day) and the chain propagator (like NO during the day).

Production of HO_x radicals is typically dominated by reactions of alkoxy (RO) radicals with O_2 , with a minor contribution from alkene ozonolysis reactions. Loss of HO_x is largely controlled by $\text{HO}_2 + \text{RO}_2$ reactions and $\text{OH} + \text{NO}_2$, while the loss of HO_2 is typically dominated by the radical propagations reactions $\text{HO}_2 + \text{NO}_3$ and $\text{HO}_2 + \text{O}_3$.

Now that the chemistry occurring in the model during the night has been described, the model sensitivity to various uncertainties can be evaluated so that the reasons for the model overprediction of NO_{3x} and underprediction of HO_2 can be investigated.

7 Sources of model uncertainties

Model calculations for RONOCO display a tendency to underpredict HO_2^* whilst overpredicting NO_3 and N_2O_5 . In this section we investigate the impact of potential sources of uncertainty on models of nighttime chemistry and composition. First we consider the impact of the timescale adopted in the model to describe physical losses of long-lived species in the model. Secondly, given the role of heterogenous uptake of N_2O_5 in determining NO_{3x} loss processes and the significant uncertainty in uptake coefficients in the literature (Brown et al., 2006, 2009, 2011; Escoreia et al., 2010; Tang et al., 2010; Badger et al., 2006; Thornton and Abbatt, 2005; Hallquist et al., 2003; Thornton et al., 2003; Kane et al., 2001; Hu and Abbatt, 1997; Fried et al., 1994; Van Doren et al., 1991; Hanson and Ravishankara, 1991; Mozurkewich and Calvert, 1998) we investigate the model sensitivity to $\gamma_{\text{N}_2\text{O}_5}$. We then focus on model uncertainties which have the potential to rectify both the model underprediction of HO_2^* and overprediction of NO_{3x} , i.e. parameters which are simultaneously sinks of NO_{3x} and sources of HO_x such as the reaction rate between NO_3 and RO_2 and the impact of missing VOCs.

[Title Page](#)[Abstract](#)[Introduction](#)[Conclusions](#)[References](#)[Tables](#)[Figures](#)[◀](#)[▶](#)[◀](#)[▶](#)[Back](#)[Close](#)[Full Screen / Esc](#)[Printer-friendly Version](#)[Interactive Discussion](#)

7.1 Impact of timescale for physical loss

As described in Sect. 4, model calculations reported here include a first-order loss process to represent continuous physical loss processes to prevent the build-up of unmeasured species in the model. In our previous work as part of the African Monsoon Multidisciplinary Analyses (AMMA) campaign we investigated the impact of the rate of physical loss on HO_x simulations (Stone et al., 2010). Results of model simulations for daytime chemistry during AMMA indicated little impact of the physical loss rate on modelled HO₂ concentrations, with the lifetimes with respect to physical loss varied between 1 h and 5 days (Stone et al., 2010). Figure 9a shows the impact of the modelled timescale for physical loss on the nighttime RONOCO simulations for HO₂ and NO_{3x}. There is little impact on modelled HO₂ or NO_{3x} on variation of the lifetime for physical loss from 12 to 48 h. Thus it does not seem likely that the simplistic treatment of deposition or mixing processes considered in the model is likely to explain the overall performance of the model.

7.2 Impact of $\gamma_{\text{N}_2\text{O}_5}$

Both laboratory and field studies of the value of $\gamma_{\text{N}_2\text{O}_5}$ are highly variable (Brown et al., 2006, 2009, 2011; Escoreia et al., 2010; Tang et al., 2010; Macintyre and Evans, 2010; Badger et al., 2006; Thornton and Abbatt, 2005; Hallquist et al., 2003; Thornton et al., 2003; Kane et al., 2001; Hu and Abbatt, 1997; Fried et al., 1994; Van Doren et al., 1991; Hanson and Ravishankara, 1991; Mozurkewich and Calvert, 1998) with values varying over several orders of magnitude (10^{-4} to > 0.1). The base model uses a fixed value of $\gamma_{\text{N}_2\text{O}_5} = 0.02$, based on the global mean value (Evans and Jacob, 2005). Figure 9b shows the impact of varying $\gamma_{\text{N}_2\text{O}_5}$ from 0 to 1 on the on the median modelled to observed ratios of HO₂ and NO_{3x}. The best fit values for NO₃ and N₂O₅ (i.e. median modelled to observed ratio closest to unity) are achieved when $\gamma_{\text{N}_2\text{O}_5} \sim 0.05$ (which is within the range of laboratory studies). However, these higher values of $\gamma_{\text{N}_2\text{O}_5}$ result in lower modelled HO₂ concentrations since the increased loss of NO_{3x} to aerosol surfaces

[Title Page](#)[Abstract](#)[Introduction](#)[Conclusions](#)[References](#)[Tables](#)[Figures](#)[◀](#)[▶](#)[◀](#)[▶](#)[Back](#)[Close](#)[Full Screen / Esc](#)[Printer-friendly Version](#)[Interactive Discussion](#)

decreases the rate of radical production from NO_3 -initiated oxidation processes and widens the gap between observed and modelled HO_2 concentrations.

Heterogeneous uptake of HO_2 was found to constitute a relatively minor loss process for HO_2 (7 % of the total) and RO_x radicals (< 2 % of the total), as discussed in Sect. 6, and there is thus little model sensitivity to γ_{HO_2} .

7.3 Impact of $k_{\text{NO}_3+\text{RO}_2}$

The reaction between peroxy (RO_2) radicals and NO_3 are central to the production of HO_2 at night and play an important role in removing NO_3 . There, have been however, very few studies of this important class of compounds (see for example Vaughan et al., 2006) compared to equivalent studies of daytime radical reactions. The MCM considers three different reactions rates for this class, one for CH_3O_2 , one for $\text{RC}(\text{O})\text{O}_2$ and one for all other RO_2 , with no temperature dependence considered and all reaction products assumed to be analogous to the corresponding reaction of the RO_2 radical with NO .

Figure 9c shows the sensitivity of the mean modelled to observed ratios of HO_2 and NO_{3x} on $k_{\text{NO}_3+\text{RO}_2}$, where all $k_{\text{NO}_3+\text{RO}_2}$ have been increased by the same factor. We find that increases in $k_{\text{NO}_3+\text{RO}_2}$ lead to increases in modelled HO_2^* and decreases in modelled NO_{3x} , but large (> 10) changes in $k_{\text{NO}_3+\text{RO}_2}$ are required to significantly improve the model success. However, there have been no measurements of the kinetics of peroxy radicals derived from NO_3 -initiated oxidation, which are significant at night, and there may be significant differences in the behaviour of peroxy radicals derived from OH - and O_3 -initiated oxidation, which are used to estimate $k_{\text{NO}_3+\text{RO}_2}$ in the model, and those derived from NO_3 -initiated oxidation. The presence of unknown VOCs, and thus of unknown RO_2 radicals, leads to further uncertainties in $k_{\text{NO}_3+\text{RO}_2}$. The available database of laboratory data concerning radical processing in nighttime atmospheres is extremely limited.

[Title Page](#)[Abstract](#)[Introduction](#)[Conclusions](#)[References](#)[Tables](#)[Figures](#)[◀](#)[▶](#)[◀](#)[▶](#)[Back](#)[Close](#)[Full Screen / Esc](#)[Printer-friendly Version](#)[Interactive Discussion](#)

7.4 Impact of VOC concentrations

Reactions of NO_3 with VOCs are important for both NO_3 loss and RO_x radical production. Previous studies have invoked unmeasured VOCs to explain both model overpredictions of NO_3 and underpredictions of HO_2 .

Figure 10 displays the comparison between modelled and observed concentrations of HO_2 , NO_3 and N_2O_5 for a model run in which the concentrations of all species containing C=C were set to zero. Compared to the base model run (Fig. 2), the run with no unsaturated hydrocarbons shows a marked increase in modelled concentrations of NO_{3x} and very little HO_2 production, demonstrating the significance of unsaturated VOCs as both a sink of NO_{3x} and a source of HO_2 . The presence of unquantified or unmeasured VOCs thus has the potential to improve model simulations for both HO_2 and NO_{3x} .

Figure 9d shows the impact of increasing the concentration of unsaturated VOCs on the mean modelled to measured ratios of HO_2 , NO_3 and N_2O_5 , represented as the increase in reactivity towards NO_3 , where the reactivity is given by $\sum k_{\text{NO}_3+\text{VOC}}[\text{VOC}]$. An increase of approximately 4 times the total observed C=C reactivity results in significant improvements to model simulations for HO_2^* and simultaneously improves the modelled NO_{3x} .

Thus significant concentrations of unmeasured VOCs during RONOCO may explain the model measurement discrepancy. Previous work using two-dimensional gas chromatography (2D-GC) in urban environments isolated and classified over 500 different VOCs not routinely measured, with significant impacts on atmospheric chemistry (Lewis et al., 2000). 2D-GC analyses of the whole air samples (WAS) collected during the RONOCO campaign have also revealed the presence of a large number of VOCs which are not routinely measured (Lidster et al., 2013). Although the 2D-GC analyses identify the presence of additional species, and, based on expected relationships between polarity and boiling point, can identify the presence of additional unsaturated VOCs, the current absence of readily available calibration standards for long-chain

[Title Page](#)[Abstract](#)[Introduction](#)[Conclusions](#)[References](#)[Tables](#)[Figures](#)[◀](#)[▶](#)[◀](#)[▶](#)[Back](#)[Close](#)[Full Screen / Esc](#)[Printer-friendly Version](#)[Interactive Discussion](#)

alkenes and other unsaturated VOCs makes full identification and quantification of such species impractical.

One class of compounds which could have a significant impact on the nighttime chemistry is monoterpenes. A model run in which α -pinene was included at a concentration equivalent to the limit of detection (131 to 280 ppt) for the proton transfer mass spectrometer (PTR-MS) onboard the BAe146 during RONOCO decreased the median modelled to observed ratios for NO_3 and N_2O_5 from 1.68 and 1.64, respectively, for the base model run to 0.76 and 0.82, respectively. Thus total monoterpenes in the 100 ppt range would significantly improve the fidelity of the NO_3 and N_2O_5 simulation. However, the median modelled to observed ratio for HO_2^* was reduced from 0.56 for the base model run to 0.34 on inclusion of α -pinene. This reduction is predominantly due to α -pinene derived RO radicals undergoing internal rearrangements to produce carbonyl compounds and NO_2 , in preference to reaction with O_2 to produce carbonyl compounds and HO_2 as exhibited by other unsaturated VOCs. Similarly, inclusion of styrene in the model at concentrations equivalent to those observed for ethylbenzene (median ~ 8 ppt) reduced the median modelled to observed ratios for NO_3 and N_2O_5 to 1.31 and 1.11, respectively, but also reduced the median modelled to observed ratio for HO_2^* to 0.29 owing to similar behaviour of styrene-derived RO_2 and RO radicals to those derived from monoterpenes. Low concentrations of species such as monoterpenes and styrene which display high reactivity towards NO_3 can thus have a significant impact on NO_{3x} concentrations, and the presence of such compounds may reduce the N_2O_5 aerosol uptake coefficient required to achieve model success for NO_{3x} , but the larger hydrocarbons appear to be less efficient at generating HO_2 and cannot fully explain the model discrepancies observed for this work.

We thus conclude that unquantified species containing C=C could reconcile model and measured NO_3 , N_2O_5 and HO_2 . However, their exact nature remains unknown. Any compound would have to be heavy enough to not be measured using the GC-FID system yet small enough not to exhibit the tendency for radical internal rearrangement which limits the ability to produce HO_2 .

Radical chemistry at night

D. Stone et al.

Title Page

Abstract

Introduction

Conclusions

References

Tables

Figures

◀

▶

◀

▶

Back

Close

Full Screen / Esc

Printer-friendly Version

Interactive Discussion



8 Future studies

The RONOCO dataset is one of the few datasets that has made extensive nighttime observations of both HO_x and NO_{3x} , particularly in regions with significant NO_x concentrations but remote from primary sources. There is a paucity of previous studies of these chemical regimes leading to uncertainty about the chemistry occurring in such chemical systems. The uncertainties found in this study could be reduced by providing direct observations of higher alkenes and terpenes at low levels. Given the high modelled RO_2 to HO_2 ratios, a measurement of RO_2 concentrations would provide a significant constraint on the chemistry. From a laboratory perspective, measurements of $\text{RO}_2 + \text{NO}_3$ rate coefficients for a variety of RO_2 radicals and under a range of temperatures and pressures would also improve our understanding of this system.

9 Conclusions

Nighttime measurements of HO_2^* , NO_3 and N_2O_5 over the UK during the RONOCO project have been compared to box model calculations simulations using the MCM. The model tends to underestimate HO_2^* , whilst overestimating NO_3 and N_2O_5 . We find that $\text{NO}_3 + \text{VOC}$ chemistry is the most significant source of RO_x radicals in the model, and that reactions of NO_3 with peroxy radicals dominate radical propagation. We observe a strong coupling between HO_2 and NO_3 at night, in both the measurements and the model calculations, although there are significant uncertainties associated with modelling of nighttime oxidation chemistry. Model simulations for NO_3 and N_2O_5 can be improved through the use of increased aerosol uptake coefficients for N_2O_5 , but the improvements for NO_3 and N_2O_5 are at the expense of model success for HO_2 . Improvements to model simulations for HO_2 , NO_3 and N_2O_5 can be achieved through the inclusion of additional unsaturated VOCs in the model. However, these missing VOCs would have to be in significant concentrations and have a significant HO_2 yield.

Title Page

Abstract

Introduction

Conclusions

References

Tables

Figures

◀

▶

◀

▶

Back

Close

Full Screen / Esc

Printer-friendly Version

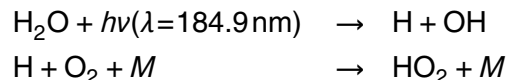
Interactive Discussion



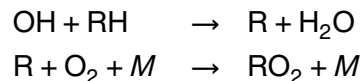
We conclude that the inclusion of appropriate $\text{NO}_3 + \text{VOC}$ and $\text{NO}_3 + \text{RO}_2$ chemistry is essential to successful model simulations of tropospheric oxidation at night.

Model treatment of potential RO_2 interferences in HO_2 measurements

Following the work of Fuchs et al. (2011), the Leeds aircraft FAGE instrument was investigated for potential interferences in measurements of HO_2 from alkene-derived RO_2 radicals. Experimental conditions will be discussed in detail by Whalley et al. (2013), and will be provided only briefly here. Interference testing was conducted using the FAGE calibration setup described by Commane et al. (2010), in which equal amounts of OH and HO_2 are produced by passing a known flow ($\sim 50 \text{ dm}^3 \text{ min}^{-1}$) of humidified ultra-high purity air (BTCA 178, BOC Special Gases) across a low pressure mercury lamp of known actinic flux:



In order to generate RO_2 radicals in the flow an excess of the parent hydrocarbon was added to the flow, such that the OH radicals produced were converted stoichiometrically to RO_2 , resulting in equal amounts of HO_2 and RO_2 in the flow:



Comparison of observed signals in the HO_2 detection cell with and without addition of the parent hydrocarbon thus enables determination of the RO_2 interference. For this work, interferences were investigated for RO_2 radicals derived from ethene giving an interference of $(39.7 \pm 4.8) \%$ for 1 : 1 HO_2 : RO_2 mixtures.

The chemistry responsible for producing RO_2 interferences in HO_2 measurements by FAGE appears to be well described by the MCM (Fuchs et al., 2011; Whalley et al.,

Title Page

Abstract

Introduction

Conclusions

References

Tables

Figures

◀

▶

◀

▶

Back

Close

Full Screen / Esc

Printer-friendly Version

Interactive Discussion



Radical chemistry at night

D. Stone et al.

Title Page

Abstract

Introduction

Conclusions

References

Tables

Figures

◀

▶

◀

▶

Back

Close

Full Screen / Esc

Printer-friendly Version

Interactive Discussion



2013), and the total potential interference in the measurements made during RONOCO were thus estimated with an MCM based box model. The box model, constrained to the characteristics of the FAGE instrument (cell pressure of 1.8 Torr; cell temperature of 260 K; NO concentration $\sim 10^{14} \text{ cm}^{-3}$) and initialised with equal amounts of HO₂ and all organic RO₂ radicals described in the MCM was run forwards in time until the modelled interferences from RO₂ radicals derived from ethene reached the experimentally derived values of 40 %. An interference factor, f , was then determined from the model output for each RO₂ radical, where f is the fractional change in the modelled HO₂ signal (i.e. the amount of OH produced) for a 1 : 1 mixture of HO₂ and RO₂. The modelled HO₂^{*} (the combination of HO₂ and potential interferences from RO₂) was subsequently determined for each time point using HO₂^{*} = HO₂ + f RO₂ for direct comparison with the FAGE measurements. Figure A1 shows the comparison between modelled HO₂^{*} and HO₂ for RONOCO, indicating that interferences during the campaign were generally small.

15 *Acknowledgements.* This work was funded by the UK Natural Environment Research Council (NE/F004664/1). The authors would like to thank ground staff, engineers, scientists and pilots involved in RONOCO for making this project a success. Airborne data were obtained using the BAe146 Atmospheric Research Aircraft (ARA) flown by Directflight Ltd. and managed by the Facility for Airborne Atmospheric Measurements (FAAM), which is a joint entity of the Natural
20 Environment Research Council (NERC) and the Met Office.

References

- Aldener, M., Brown, S. S., Stark, H., Williams, E. J., Lerner, B. M., Kuster, W. C., Goldan, P. D., Quinn, P. K., Bates, T. S., Fehsenfeld, F. C., and Ravishankara, A. R.: Reactivity and loss mechanisms of NO₃ and N₂O₅ in a polluted marine environment: results from in situ measurements during New England Air Quality Study 2002, *J. Geophys. Res.*, 111, D23S73, doi:10.1029/2006JD007252, 2006.
- 25 Aliwell, S. R. and Jones, R. L.: Measurements of tropospheric NO₃ at midlatitude, *J. Geophys. Res. Atmos.*, 103, D5, 5719–5727, 1998.

Radical chemistry at night

D. Stone et al.

Title Page

Abstract

Introduction

Conclusions

References

Tables

Figures

◀

▶

◀

▶

Back

Close

Full Screen / Esc

Printer-friendly Version

Interactive Discussion



- Allan, B. J., Plane, J. M. C., Coe, H., and Shillito, J.: Observations of NO_3 concentration profiles in the troposphere, *J. Geophys. Res.*, 107, doi:10.1029/2002JD002112, 2002.
- Badger, C. L., Griffiths, P. T., George, I., Abbatt, J. P. D., and Cox, R. A.: Reactive uptake of N_2O_5 by aerosol particles containing mixtures of humic acid and ammonium sulfate, *J. Phys. Chem. A.*, 110, 6986–6994, 2006.
- Bloss, W. J., Gravestock, T. J., Heard, D. E., Ingham, T., Johnson, G. P., and Lee, J. D.: Application of a compact all solid-state laser system to the in situ detection of atmospheric OH, HO_2 , NO and IO by laser-induced fluorescence, *J. Environ. Monit.*, 5, 21–28, 2003.
- Brough, N., Reeves, C. E., Penkett, S. A., Stewart, D. J., Dewey, K., Kent, J., Barjat, H., Monks, P. S., Ziereis, H., Stock, P., Huntrieser, H., and Schlager, H.: Intercomparison of aircraft instruments on board the C-130 and Falcon 20 over southern Germany during EXPORT 2000, *Atmos. Chem. Phys.*, 3, 2127–2138, doi:10.5194/acp-3-2127-2003, 2003.
- Brown, S. S. and Stutz, J.: Nighttime radical observations and chemistry, *Chem. Soc. Rev.*, 41, 6405–6447, 2012.
- Brown, S. S., Stark, H., and Ravishankara, A. R.: Applicability of the steady state approximation to the interpretation of atmospheric observations of NO_3 and N_2O_5 , *J. Geophys. Res.*, 108, doi:10.1029/2003JD003407, 2003.
- Brown, S. S., Dibb, J. E., Stark, H., Aldener, M., Vozella, M., Whitlow, S., Williams, E. J., Lerner, B. M., Jakoubek, R., Middlebrook, A. M., DeGouw, J. A., Warneke, C., Goldan, P. D., Kuster, W. C., Angevine, W. M., Sueper, D. T., Quinn, P. K., Bates, T. S., Meagher, J. F., Fehsenfeld, F. C., and Ravishankara, A. R.: Nighttime removal of NO_x in the summer marine boundary layer, *Geophys. Res. Lett.*, 31, L07108, doi:10.1029/2004GL019412, 2004.
- Brown, S. S., Ryerson, T. B., Wollny, A. G., Brock, C. A., Peltier, R., Sullivan, A. P., Weber, R. J., Dube, W. P., Trainer, M., Meagher, J. F., Fehsenfeld, F. C., and Ravishankara, A. R.: Variability in nocturnal nitrogen oxide processing and its role in regional air quality, *Science*, 311, 67–70, 2006.
- Brown, S. S., Dubé, W. P., Osthoff, H. D., Wolfe, D. E., Angevine, W. M., and Ravishankara, A. R.: High resolution vertical distributions of NO_3 and N_2O_5 through the nocturnal boundary layer, *Atmos. Chem. Phys.*, 7, 139–149, doi:10.5194/acp-7-139-2007, 2007.
- Brown, S. S., deGouw, J. A., Warneke, C., Ryerson, T. B., Dubé, W. P., Atlas, E., Weber, R. J., Peltier, R. E., Neuman, J. A., Roberts, J. M., Swanson, A., Flocke, F., McKeen, S. A., Brioude, J., Sommariva, R., Trainer, M., Fehsenfeld, F. C., and Ravishankara, A. R.: Nocturnal isoprene oxidation over the Northeast United States in summer and its impact on

Radical chemistry at night

D. Stone et al.

[Title Page](#)[Abstract](#)[Introduction](#)[Conclusions](#)[References](#)[Tables](#)[Figures](#)[◀](#)[▶](#)[◀](#)[▶](#)[Back](#)[Close](#)[Full Screen / Esc](#)[Printer-friendly Version](#)[Interactive Discussion](#)

reactive nitrogen partitioning and secondary organic aerosol, *Atmos. Chem. Phys.*, 9, 3027–3042, doi:10.5194/acp-9-3027-2009, 2009.

Brown, S. S., Dube, W. P., Peischl, J., Ryerson, T. B., Atlas, E., Warneke, C., de Gouw, J. A., Hekkert, St. L., Brock, C. A., Flocke, F., Trainer, M., Parrish, D. D., Fehsenfeld, F. C., and Ravishankara, A. R.: Budgets for nocturnal VOC oxidation by nitrate radicals aloft during the 2006 Texas Air Quality Study, *J. Geophys. Res.*, 116, D24305, doi:10.1029/2011JD016544, 2011.

Carslaw, N., Carpenter, L. J., Plane, J. M. C., Allan, B. J., Burgess, R. A., Clemitshaw, K. C., Coe, H., and Penkett, S. A.: Simultaneous observations of nitrate and peroxy radicals in the marine boundary layer, *J. Geophys. Res.*, 102, 18917–18933, 1997.

Commane, R., Floquet, C. F. A., Ingham, T., Stone, D., Evans, M. J., and Heard, D. E.: Observations of OH and HO₂ radicals over West Africa, *Atmos. Chem. Phys.*, 10, 8783–8801, doi:10.5194/acp-10-8783-2010, 2010.

Dari-Salisburgo, C., Di Carlo, P., Giammaria, F., Kajii, Y., and D'Altorio, A.: Laser induced fluorescence instrument for NO₂ measurements: observations at a central Italy background site, *Atmos. Environ.*, 43, 970–977, 2009.

Di Carlo, P., Aruffo, E., Busilacchio, M., Giammaria, F., Dari-Salisburgo, C., Biancofiore, F., Visconti, G., Lee, J., Moller, S., Reeves, C. E., Bauguitte, S., Forster, G., Jones, R. L., and Ouyang, B.: Aircraft based four-channel thermal dissociation laser induced fluorescence instrument for simultaneous measurements of NO₂, total peroxy nitrate, total alkyl nitrate, and HNO₃, *Atmos. Meas. Tech. Discuss.*, 5, 8759–8787, doi:10.5194/amtd-5-8759-2012, 2012.

Ehhalt, D. H. and Rohrer, F.: The tropospheric cycle of H₂: a critical review, *Tellus B*, 61, 500–535, 2009.

Emmerson, K. M. and Carslaw, N.: Night-time radical chemistry during the TORCH campaign, *Atmos. Environ.*, 43, 3220–3226, 2009.

Emmerson, K. M. and Evans, M. J.: Comparison of tropospheric gas-phase chemistry schemes for use within global models, *Atmos. Chem. Phys.*, 9, 1831–1845, doi:10.5194/acp-9-1831-2009, 2009.

Escoreia, E. N., Sjostedt, S. J., and Abbatt, J. P. D.: Kinetics of N₂O₅ hydrolysis on secondary organic aerosol and mixed ammonium bisulfate-secondary organic aerosol particles, *J. Phys. Chem. A*, 114, 13113–13121, 2010.

Radical chemistry at night

D. Stone et al.

Title Page

Abstract

Introduction

Conclusions

References

Tables

Figures

◀

▶

◀

▶

Back

Close

Full Screen / Esc

Printer-friendly Version

Interactive Discussion



- Evans, M. J. and Jacob, D. J.: Impact of new laboratory studies of N_2O_5 hydrolysis on global model budgets of tropospheric nitrogen oxides, ozone, and OH, *Geophys. Res. Lett.*, 32, 1–4, 2005.
- Faloon, I., Tan, D., Brune, W., Hurst, J., Barkley, D., Couch, T. L., Shepson, P., Apel, E., Riemer, D., Thornberry, T., Carroll, M. A., Sillman, S., Keeler, G. J., Sagady, J., Hooper, D., and Paterson, K.: Nighttime observations of anomalously high levels of hydroxyl radicals above a deciduous forest canopy, *J. Geophys. Res. Atmos.*, 106, 24315–24333, 2001.
- Fleming, Z. L., Monks, P. S., Rickard, A. R., Heard, D. E., Bloss, W. J., Seakins, P. W., Still, T. J., Sommariva, R., Pilling, M. J., Morgan, R., Green, T. J., Brough, N., Mills, G. P., Penkett, S. A., Lewis, A. C., Lee, J. D., Saiz-Lopez, A., and Plane, J. M. C.: Peroxy radical chemistry and the control of ozone photochemistry at Mace Head, Ireland during the summer of 2002, *Atmos. Chem. Phys.*, 6, 2193–2214, doi:10.5194/acp-6-2193-2006, 2006.
- Fried, A., Henry, B. E., Calvert, J. G., and Mozurkewich, M.: The reaction probability of N_2O_5 with sulfuric acid aerosols probed by the heterogeneous hydrolysis of N_2O_5 , *Geophys. Res. Lett.*, 99, 3517–3532, 1994.
- Fuchs, H., Bohn, B., Hofzumahaus, A., Holland, F., Lu, K. D., Nehr, S., Rohrer, F., and Wahner, A.: Detection of HO_2 by laser-induced fluorescence: calibration and interferences from RO_2 radicals, *Atmos. Meas. Tech.*, 4, 1209–1225, doi:10.5194/amt-4-1209-2011, 2011.
- Gerbig, C., Schmitgen, S., Kley, D., Volz-Thomas, A., Dewey, K., and Haaks, D.: An improved fast-response vacuum UV resonance fluorescence CO instrument, *J. Geophys. Res. Atmos.*, 104, 1699–1704, 1999.
- Geyer, A., Bachmann, K., Hofzumahaus, A., Holland, F., Konrad, S., Klupfel, T., Patz, H.-W., Perner, D., Mihelcic, D., Schafer, H.-J., Volz-Thomas, A., and Platt, U.: Nighttime formation of peroxy and hydroxyl radicals during the BERLIOZ campaign: observations and modeling studies, *J. Geophys. Res.*, 108, doi:10.1029/2001JD000656, 2003.
- GLOBALVIEW-CH₄, 2010–2011: Cooperative Atmospheric Data Integration Project – Methane. CD-ROM, also available on Internet via anonymous FTP to ftp://ftp.cmdl.noaa.gov/ccg/ch4/, path: ccg/CH4/GLOBALVIEW, 2010–2011, last accessed: 24 May 2011, NOAA ESRL, Boulder, Colorado, 2011.
- Hallquist, M., Stewart, D. J., Stephenson, S. K., and Cox, R. A.: Hydrolysis of N_2O_5 on sub-micron sulfate aerosols, *Phys. Chem. Chem. Phys.*, 5, 3453–3463, 2003.
- Hanson, D. R. and Ravishankara, A. R.: The reaction probabilities of ClONO_2 and N_2O_5 on 40 to 75 % sulfuric acid solutions, *J. Geophys. Res.*, 96, 17307–17314, 1991.

Radical chemistry at night

D. Stone et al.

Title Page

Abstract

Introduction

Conclusions

References

Tables

Figures

◀

▶

◀

▶

Back

Close

Full Screen / Esc

Printer-friendly Version

Interactive Discussion



- Heard, D. E. and Pilling, M. J.: Measurement of OH and HO₂ in the troposphere, *Chem. Reviews*, 103, 5163–5198, 2003.
- Hopkins, J. R., Lewis, A. C., and Read, K. A.: A two-column method for long-term monitoring of non-methane hydrocarbons (NMHCs) and oxygenated volatile organic compounds (oVOCs), *J. Environ. Monit.*, 5, 8–13, 2003.
- Hu, J. H. and Abbatt, J. P. D.: Reaction probabilities for N₂O₅ hydrolysis on sulfuric acid and ammonium sulfate aerosols at room temperature, *J. Phys. Chem. A*, 101, 871–878, 1997.
- Jenkin, M. E., Saunders, S. M., Wagner, V., and Pilling, M. J.: Protocol for the development of the Master Chemical Mechanism, MCM v3 (Part B): tropospheric degradation of aromatic volatile organic compounds, *Atmos. Chem. Phys.*, 3, 181–193, doi:10.5194/acp-3-181-2003, 2003.
- Johnson, D. and Marston, G.: The gas-phase ozonolysis of unsaturated volatile organic compounds in the troposphere, *Chem. Soc. Rev.*, 37, 699–716, 2008.
- Kanaya, Y., Sadanaga, Y., Matsumoto, J., Sharma, U. K., Hirokawa, J., Kajii, Y., and Akimoto, H.: Nighttime observation of the HO₂ radical by an LIF instrument at Oki island, Japan, and its possible origins, *Geophys. Res. Lett.*, 26, 2179–2182, 1999.
- Kanaya, Y., Nakamura, K., Kato, S., Matsumoto, J., Tanimoto, H., and Akimoto, H.: Nighttime variations in HO₂ radical mixing ratios at Rishiri Island observed with elevated monoterpene mixing ratios, *Atmos. Environ.*, 36, 4929–4940, 2002.
- Kanaya, Y., Cao, R., Kato, S., Miyakawa, Y., Kajii, Y., Tanimoto, H., Yokouchi, Y., Mochida, M., Kawamura, K., and Akimoto, H.: Chemistry of OH and HO₂ radicals observed at Rishiri Island, Japan, in September 2003: missing daytime sink of HO₂ and positive nighttime correlations with monoterpenes, *J. Geophys. Res.*, 112, D11308, doi:10.1029/2006JD007987, 2007.
- Kanaya, Y., Cao, R., Akimoto, H., Fukuda, M., Komazaki, Y., Yokouchi, Y., Koike, M., Tanimoto, H., Takegawa, N., and Kondo, Y.: Urban photochemistry in central Tokyo: 1. Observed and modeled OH and HO₂ radical concentrations during the winter and summer of 2004, *J. Geophys. Res.*, 112, D21312, doi:10.1029/2007JD008670, 2007.
- Kane, S. M., Caloz, F., and Leu, M.-T.: Heterogeneous uptake of gaseous N₂O₅ by (NH₄)₂SO₄, NH₄HSO₄ and H₂SO₄ aerosols, *J. Phys. Chem.*, 105, 6465–6470, 2001.
- Kennedy, O. J., Ouyang, B., Langridge, J. M., Daniels, M. J. S., Bauguitte, S., Freshwater, R., McLeod, M. W., Ironmonger, C., Sendall, J., Norris, O., Nightingale, R., Ball, S. M., and Jones, R. L.: An aircraft based three channel broadband cavity enhanced absorption spec-

Radical chemistry at night

D. Stone et al.

Title Page

Abstract

Introduction

Conclusions

References

Tables

Figures

◀

▶

◀

▶

Back

Close

Full Screen / Esc

Printer-friendly Version

Interactive Discussion



trometer for simultaneous measurements of NO₃, N₂O₅ and NO₂, Atmos. Meas. Tech., 4, 1759–1776, doi:10.5194/amt-4-1759-2011, 2011.

Lewis, A. C., Carslaw, N., Marriott, P. J., Kinghorn, R. M., Morrison, P., Lee, A. L., Bartle, K. D., and Pilling, M. J.: A larger pool of ozone-forming carbon compounds in urban atmospheres, Nature, 405, 778–781, 2000.

Lidster, R. T., Hamilton, J. F., Lee, J. D., Lewis, A. C., Hopkins, J. R., Punjabi, S., Rickard, A. R., and Young, J.: Investigation of the impact of large aromatics on OH reactivity over the UK using comprehensive two-dimensional gas chromatography coupled to time of flight mass spectrometry (GC-GC-TOFMS), in preparation, 2013.

Macintyre, H. L. and Evans, M. J.: Sensitivity of a global model to the uptake of N₂O₅ by tropospheric aerosol, Atmos. Chem. Phys., 10, 7409–7414, doi:10.5194/acp-10-7409-2010, 2010.

Macintyre, H. L. and Evans, M. J.: Parameterisation and impact of aerosol uptake of HO₂ on a global tropospheric model, Atmos. Chem. Phys., 11, 10965–10974, doi:10.5194/acp-11-10965-2011, 2011.

Malkin, T. L., Goddard, A., Heard, D. E., and Seakins, P. W.: Measurements of OH and HO₂ yields from the gas phase ozonolysis of isoprene, Atmos. Chem. Phys., 10, 1441–1459, doi:10.5194/acp-10-1441-2010, 2010.

Martinez, M., Harder, H., Kovacs, T. A., Simpas, J. B., Bassis, J., Leshner, R., Brune, W. H., Frost, G. J., Williams, E. J., Stroud, C. A., Jobson, B. T., Roberts, J. M., Hall, S. R., Shetter, R. E., Wert, B., Fried, A., Alicke, B., Stutz, J., Young, V. L., White, A. B., and Zamora, R. J.: OH and HO₂ concentrations, sources, and loss rates during the Southern Oxidants Study in Nashville, Tennessee, summer 1999, J. Geophys. Res., 108, doi:10.1029/2003JD003551, 2003.

Mihelcic, D., Klemp, D., Musgen, P., Patz, H. W., and Volz-Thomas, A.: Simultaneous measurements of peroxy and nitrate radicals at Schauinsland, J. Atmos. Chem., 16, 313–335, 1993.

Mozurkewich, M. and Calvert, J. G.: Reaction probability of N₂O₅ on aqueous aerosols, J. Geophys. Res., 93, 15889–15896, 1988.

Novelli, P. C., Lang, P. M., Masarie, K. A., Hurst, D. F., Myers, R., and Elkins, J. W.: Molecular hydrogen in the troposphere: global distribution and budget, J. Geophys. Res., 104, 30427–30444, 1999.

Radical chemistry at night

D. Stone et al.

Title Page

Abstract

Introduction

Conclusions

References

Tables

Figures

◀

▶

◀

▶

Back

Close

Full Screen / Esc

Printer-friendly Version

Interactive Discussion



- Platt, U., Perner, D., Winer, A. M., Harris, G. W., and Pitts, J. N.: Detection of NO_3 in the polluted troposphere by differential optical absorption, *Geophys. Res. Lett.*, 7, 89–92, 1980.
- Povey, I., South, A., de Roodenbeke, A., Hill, C., Freshwater, R., and Jones, R.: A broadband lidar for the measurement of tropospheric constituent profiles from the ground, *J. Geophys. Res. Atmos.*, 103, 3369–3380, 1998.
- Ravishankara, A. R.: Heterogeneous and multiphase chemistry in the troposphere, *Science*, 276, 1058–1065, 1997.
- Ren, X., Harder, H., Martinez, M., Leshner, R. L., Olliger, A., Simpas, J. B., Brune, W. H., Schwab, J. J., Demerjian, K. L., He, Y., Zhou, X., and Gao, H.: OH and HO_2 Chemistry in the urban atmosphere of New York City, *Atmos. Environ.*, 37, 3639–3651, 2003.
- Ren, X., Brune, W. H., Cantrell, C., Edwards, G. D., Shirley, T., Metcalf, A. R., and Leshner, R. L.: Hydroxyl and peroxy radical chemistry in a rural area of central Pennsylvania: observations and model comparisons, *J. Atmos. Chem.*, 52, 231–257, 2005.
- Ren, X., Brune, W. H., Mao, J., Mitchell, M. J., Leshner, R. L., Simpas, J. B., Metcalf, A. R., Schwab, J. J., Cai, C., Li, Y., Demerjian, K. L., Felton, H. D., Boynton, G., Adams, A., Perry, J., He, Y., Zhou, X., and Hou, J.: Behavior of OH and HO_2 in the winter atmosphere in New York City, *Atmos. Environ.*, 40, S252–S263, 2006.
- Salisbury, G., Rickard, A. R., Monks, P. S., Allan, B. J., Bauguitte, S., Penkett, S. A., Carslaw, N., Lewis, A. C., Creasey, D. J., Heard, D. E., Jacobs, P. J., and Lee, J. D.: Production of peroxy radicals at night via reactions of ozone and the nitrate radical in the marine boundary layer, *J. Geophys. Res.*, 106, 12669–12687, 2001.
- Sandu, A. and Sander, R.: Technical note: Simulating chemical systems in Fortran90 and Matlab with the Kinetic PreProcessor KPP-2.1, *Atmos. Chem. Phys.*, 6, 187–195, doi:10.5194/acp-6-187-2006, 2006.
- Saunders, S. M., Jenkin, M. E., Derwent, R. G., and Pilling, M. J.: Protocol for the development of the Master Chemical Mechanism, MCM v3 (Part A): tropospheric degradation of non-aromatic volatile organic compounds, *Atmos. Chem. Phys.*, 3, 161–180, doi:10.5194/acp-3-161-2003, 2003.
- Sommariva, R., Bloss, W. J., Brough, N., Carslaw, N., Flynn, M., Haggerstone, A.-L., Heard, D. E., Hopkins, J. R., Lee, J. D., Lewis, A. C., McFiggans, G., Monks, P. S., Penkett, S. A., Pilling, M. J., Plane, J. M. C., Read, K. A., Saiz-Lopez, A., Rickard, A. R., and Williams, P. I.: OH and HO_2 chemistry during NAMBLEX: roles of oxygenates, halogen ox-

Radical chemistry at night

D. Stone et al.

Title Page

Abstract

Introduction

Conclusions

References

Tables

Figures

◀

▶

◀

▶

Back

Close

Full Screen / Esc

Printer-friendly Version

Interactive Discussion



ides and heterogeneous uptake, *Atmos. Chem. Phys.*, 6, 1135–1153, doi:10.5194/acp-6-1135-2006, 2006.

Sommariva, R., Pilling, M. J., Bloss, W. J., Heard, D. E., Lee, J. D., Fleming, Z. L., Monks, P. S., Plane, J. M. C., Saiz-Lopez, A., Ball, S. M., Bitter, M., Jones, R. L., Brough, N., Penkett, S. A., Hopkins, J. R., Lewis, A. C., and Read, K. A.: Night-time radical chemistry during the NAM-BLEX campaign, *Atmos. Chem. Phys.*, 7, 587–598, doi:10.5194/acp-7-587-2007, 2007.

Sommariva, R., Osthoff, H. D., Brown, S. S., Bates, T. S., Baynard, T., Coffman, D., de Gouw, J. A., Goldan, P. D., Kuster, W. C., Lerner, B. M., Stark, H., Warneke, C., Williams, E. J., Fehsenfeld, F. C., Ravishankara, A. R., and Trainer, M.: Radicals in the marine boundary layer during NEAQS 2004: a model study of day-time and night-time sources and sinks, *Atmos. Chem. Phys.*, 9, 3075–3093, doi:10.5194/acp-9-3075-2009, 2009.

South, A. M., Povey, I. M., and Jones, R. L.: Broadband lidar measurements of tropospheric water vapor profiles, *J. Geophys. Res. Atmos.*, 103, 31191–31202, 1998.

Stone, D., Evans, M. J., Commane, R., Ingham, T., Floquet, C. F. A., McQuaid, J. B., Brookes, D. M., Monks, P. S., Purvis, R., Hamilton, J. F., Hopkins, J., Lee, J., Lewis, A. C., Stewart, D., Murphy, J. G., Mills, G., Oram, D., Reeves, C. E., and Heard, D. E.: HO_x observations over West Africa during AMMA: impact of isoprene and NO_x, *Atmos. Chem. Phys.*, 10, 9415–9429, doi:10.5194/acp-10-9415-2010, 2010.

Stone, D., Evans, M. J., Edwards, P. M., Commane, R., Ingham, T., Rickard, A. R., Brookes, D. M., Hopkins, J., Leigh, R. J., Lewis, A. C., Monks, P. S., Oram, D., Reeves, C. E., Stewart, D., and Heard, D. E.: Isoprene oxidation mechanisms: measurements and modelling of OH and HO₂ over a South-East Asian tropical rainforest during the OP3 field campaign, *Atmos. Chem. Phys.*, 11, 6749–6771, doi:10.5194/acp-11-6749-2011, 2011.

Stone, D., Whalley, L. K., and Heard, D. E.: Tropospheric OH and HO₂ radicals: field measurements and model comparisons, *Chem. Soc. Rev.*, 41, 6348–6404, 2012.

Stutz, J., Alicke, B., Ackermann, R., Geyer, A., White, A., and Williams, E.: Vertical profiles of NO₃, N₂O₅, O₃, and NO_x in the nocturnal boundary layer: 1. Observations during the Texas Air Quality Study 2000, *J. Geophys. Res. Atmos.*, 109, D12306, doi:10.1029/2003JD004209, 2004.

Stutz, J., Wong, K. W., Lawrence, L., Ziemba, L., Flynn, J. H., Rappengluck, B., and Lefer, B.: Nocturnal NO₃ radical chemistry in Houston, TX, *Atmos. Environ.*, 44, 4099–4106, 2010.

Radical chemistry at night

D. Stone et al.

Title Page

Abstract

Introduction

Conclusions

References

Tables

Figures

◀

▶

◀

▶

Back

Close

Full Screen / Esc

Printer-friendly Version

Interactive Discussion



Tang, M. J., Thieser, J., Schuster, G., and Crowley, J. N.: Uptake of NO_3 and N_2O_5 to Saharan dust, ambient urban aerosol and soot: a relative rate study, *Atmos. Chem. Phys.*, 10, 2965–2974, doi:10.5194/acp-10-2965-2010, 2010.

Thornton, J. and Abbatt, J. P. D.: Measurements of HO_2 uptake to aqueous aerosol: mass accommodation coefficients and net reactive loss, *J. Geophys. Res.*, 110, D08309, doi:10.1029/2004JD005402, 2005.

Thornton, J. A., Braban, C. F., and Abbatt, J. P. D.: N_2O_5 hydrolysis on sub-micron organic aerosols: the effect of relative humidity, particle phase, and particle size, *Phys. Chem. Chem. Phys.*, 5, 4593–4603, 2003.

Van Doren, J. M., Watson, L. R., Davidovits, P., Worsnop, D. R., Zahniser, M. S., and Kolb, C. E.: Uptake of N_2O_5 and HNO_3 by aqueous sulfuric acid droplets, *J. Phys. Chem.*, 95, 1684–1689, 1991.

Vaughan, S., Canosa-Mas, C. E., Pfrang, C., Shallcross, D. E., Watson, L., and Wayne, R. P.: Kinetic studies of reactions of the nitrate radical (NO_3) with peroxy radicals (RO_2): an indirect source of OH at night?, *Phys. Chem. Chem. Phys.*, 8, 3749–3760, 2006.

Volkamer, R., Sheehy, P., Molina, L. T., and Molina, M. J.: Oxidative capacity of the Mexico City atmosphere – Part 1: A radical source perspective, *Atmos. Chem. Phys.*, 10, 6969–6991, doi:10.5194/acp-10-6969-2010, 2010.

Walker, H. M., Stone, D., Ingham, T., Vaughan, S., Ouyang, B., Kennedy, O., McCleod, M., Jones, R. L., Hopkins, J., Punjabi, S., Lewis, A. C., and Heard, D. E.: Nighttime measurements of HO_x during the RONOCO project, in preparation, 2013.

Warneke, C., de Gouw, J. A., Goldan, P. D., Kuster, W. C., Williams, E. J., Lerner, B. M., Jakoubek, R., Brown, S. S., Stark, H., Aldener, M., Ravishankara, A. R., Roberts, J. M., Marchewka, M., Bertman, S., Sueper, D. T., McKeen, S. A., Meagher, J. F., and Fehsenfeld, F. C.: Comparison of daytime and nighttime oxidation of biogenic and anthropogenic VOCs along the New England coast in summer during New England Air Quality Study 2002, *J. Geophys. Res.*, 109, D10309, doi:10.1029/2003JD004424, 2004.

Wayne, R. P., Barnes, I., Biggs, P., Burrows, J. P., Canosa-Mas, C. E., Hjorth, J., Le Bras, G., Moortgat, G. K., Perner, D., Poulet, G., Restelli, G., and Sidebottom, H.: The nitrate radical – physics, chemistry and the atmosphere, *Atmos. Environ.*, 25, 1, 1–203, 1991.

Whalley, L. K., Lewis, A. C., McQuaid, J. B., Purvis, R. M., Lee, J. D., Stemmler, K., Zellweger, C., and Ridgeon, P.: Two high-speed, portable GC systems designed for the mea-

surement of non-methane hydrocarbons and PAN: results from the Jungfraujoch High Altitude Observatory, J. Env. Monit., 6, 3, 234–241, 2004.
Whalley, L. K., Blitz, M. A., Seakins, P. W., and Heard, D. E.: The sensitivity of Laser Induced Fluorescence instruments to an interference from RO₂ radicals, in preparation, 2013.

ACPD

13, 9519–9566, 2013

Radical chemistry at night

D. Stone et al.

Title Page

Abstract

Introduction

Conclusions

References

Tables

Figures

⏪

⏩

◀

▶

Back

Close

Full Screen / Esc

Printer-friendly Version

Interactive Discussion



Radical chemistry at night

D. Stone et al.

Title Page

Abstract

Introduction

Conclusions

References

Tables

Figures

◀

▶

◀

▶

Back

Close

Full Screen / Esc

Printer-friendly Version

Interactive Discussion



Table 1. Supporting measurements made onboard the BAe146 aircraft during the RONOCO project and used in the model analysis presented here.

Species measured	Technique
CO	Aero Laser AL5002 Fast Carbon Monoxide Monitor (Gerbig et al., 1999).
O ₃	TECO 49C UV absorption.
NO, NO ₂ ^a	FAAM fast NO _x instrument; TECO 42C analyser using heated Molybdenum filament to convert NO ₂ to NO with detection of NO by chemiluminescence (Brough et al., 2003).
NO ₂ ^a , ΣANs, ΣPNs	Thermal decomposition of ΣANs and ΣPNs to NO ₂ ; detection of NO ₂ by laser-induced fluorescence (LIF) (Dari-Salisburgo et al., 2009; Di Carlo et al., 2012).
PAN	Gas chromatography with electron capture detection (Whalley et al., 2004).
VOCs	Gas chromatography with flame ionisation detection (GC-FID) (Hopkins et al., 2006).
Aerosol surface area ^b	Scanning mobility particle sizer (SMPS) for particles of diameter 20–350 nm.

^a The NO₂ measurements used to constrain the model were made by the LIF instrument (Dari-Salisburgo et al., 2009; Di Carlo et al., 2012). ΣANs = sum of alkyl nitrates; ΣPNs = sum of peroxy nitrates; PAN = peroxy acetyl nitrate; VOCs = volatile organic compounds.

^b Aerosol surface area is estimated for ambient relative humidity based on the measured dry size distribution and composition.

Table 2. Summary of inputs to the model. Zero values indicate measurements below the instrumental limits of detection.

Species	Mean $\pm 1\sigma$	Median	Range
O ₃ /ppb	37.0 \pm 8.1	35.5	11–63
CO/ppb	110.4 \pm 27.1	99.9	71–250
H ₂ O/ppm	10418 \pm 2425	10491	178–15509
NO ₂ /ppt	1614.4 \pm 1749.2	946.7	66–14570
NO/ppt	24.6 \pm 278.9	0	0–4501
ethane/ppt	1109.5 \pm 882.0	940.8	0–3208
propane/ppt	414.0 \pm 416.5	235.9	0–1770
<i>iso</i> -butane/ppt	94.4 \pm 91.3	73.0	0–372
<i>n</i> -butane/ppt	171.7 \pm 162.2	140.8	0–726
<i>iso</i> -pentane/ppt	80.9 \pm 139.6	70.5	0–2176
<i>n</i> -pentane/ppt	50.4 \pm 57.1	38.4	0–455
methylpentanes/ppt	28.3 \pm 31.2	21.3	0–224
<i>n</i> -hexane/ppt	17.0 \pm 18.3	11.9	0–135
<i>n</i> -heptane/ppt	6.9 \pm 10.1	5.7	0–146
<i>n</i> -octane/ppt	2.6 \pm 4.5	0	0–45
ethene/ppt	130.5 \pm 121.2	117.6	0–590
propene/ppt	30.9 \pm 45.4	12.0	0–239
acetylene/ppt	158.9 \pm 161.0	96.8	0–516
<i>trans</i> -2-butene/ppt	3.2 \pm 2.1	3.8	0–10
1-butene/ppt	6.7 \pm 7.7	5.5	0–75
<i>iso</i> -butene/ppt	5.4 \pm 8.4	4.9	0–137
<i>cis</i> -2-butene/ppt	0.1 \pm 0.6	0	0–7
1,3-butadiene/ppt	2.8 \pm 17.1	0	0–230
<i>trans</i> -2-pentene/ppt	0.1 \pm 0.7	0	0–11
1-pentene/ppt	0.9 \pm 2.5	0	0–24
isoprene/ppt	0.9 \pm 3.2	0	0–40
benzene/ppt	47.9 \pm 58.7	21.1	0–458
toluene/ppt	40.5 \pm 57.1	34.0	0–773
ethylbenzene/ppt	8.5 \pm 13.3	6.0	0–178
<i>m</i> -xylene/ppt	18.1 \pm 42.1	6.4	0–693
<i>o</i> -xylene/ppt	6.1 \pm 17.2	0	0–268
methacrolein/ppt	7.3 \pm 27.9	0	0–325
acetone/ppt	444.0 \pm 616.0	257.9	0–8073
PAN/ppt	31.2 \pm 44.2	19.0	0–234

Radical chemistry at night

D. Stone et al.

Title Page

Abstract

Introduction

Conclusions

References

Tables

Figures

◀

▶

◀

▶

Back

Close

Full Screen / Esc

Printer-friendly Version

Interactive Discussion



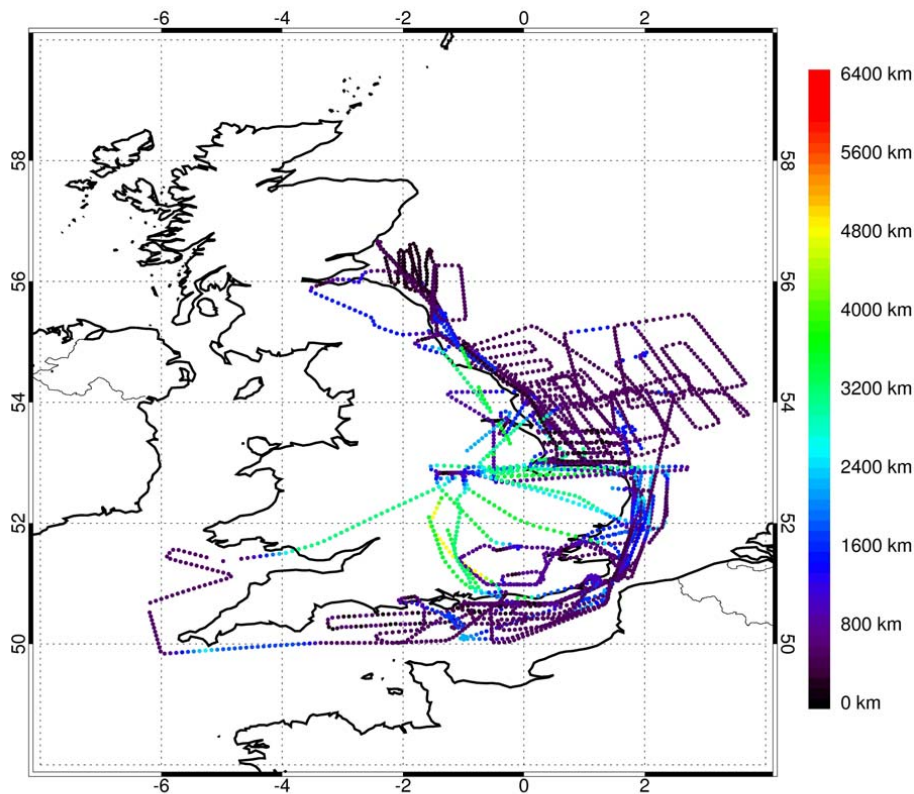


Fig. 1. Locations of the BAe146 aircraft during the RONOCO campaign for which measurements of HO_2^* and NO_3 or N_2O_5 are available, coloured by altitude.

Radical chemistry at night

D. Stone et al.

Title Page

Abstract Introduction

Conclusions References

Tables Figures

◀ ▶

◀ ▶

Back Close

Full Screen / Esc

Printer-friendly Version

Interactive Discussion



Radical chemistry at night

D. Stone et al.

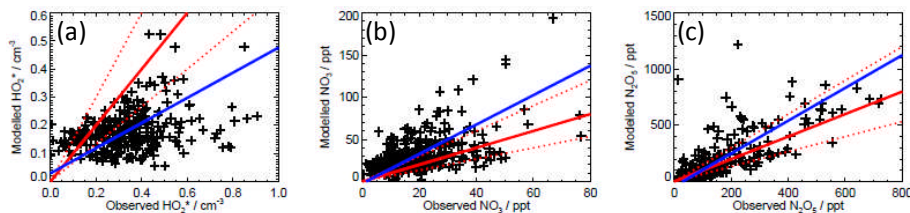


Fig. 2. Comparison of modelled and observed concentrations of **(a)** HO_2^* , **(b)** NO_3 and **(c)** N_2O_5 for the base MCM model run. In each plot, the solid red line indicates the 1 : 1 line, with 50 % limits given by the broken red lines. The best fit lines are shown in blue, and are described by $[\text{HO}_2^*]_{\text{mod}} = \{(0.45 \pm 0.07) \times [\text{HO}_2^*]_{\text{obs}}\} + (2.95 \pm 2.23) \times 10^6 \text{ cm}^{-3}$ ($r^2 = 0.10$), $[\text{NO}_3]_{\text{mod}} = \{(1.75 \pm 0.17) \times [\text{NO}_3]_{\text{obs}}\} - (2.33 \pm 3.61) \text{ ppt}$ ($r^2 = 0.29$) and $[\text{N}_2\text{O}_5]_{\text{mod}} = \{(1.46 \pm 0.12) \times [\text{N}_2\text{O}_5]_{\text{obs}}\} - (42.43 \pm 19.65) \text{ ppt}$ ($r^2 = 0.64$).

Title Page

Abstract

Introduction

Conclusions

References

Tables

Figures

◀

▶

◀

▶

Back

Close

Full Screen / Esc

Printer-friendly Version

Interactive Discussion



Radical chemistry at night

D. Stone et al.

Title Page

Abstract

Introduction

Conclusions

References

Tables

Figures

◀

▶

◀

▶

Back

Close

Full Screen / Esc

Printer-friendly Version

Interactive Discussion

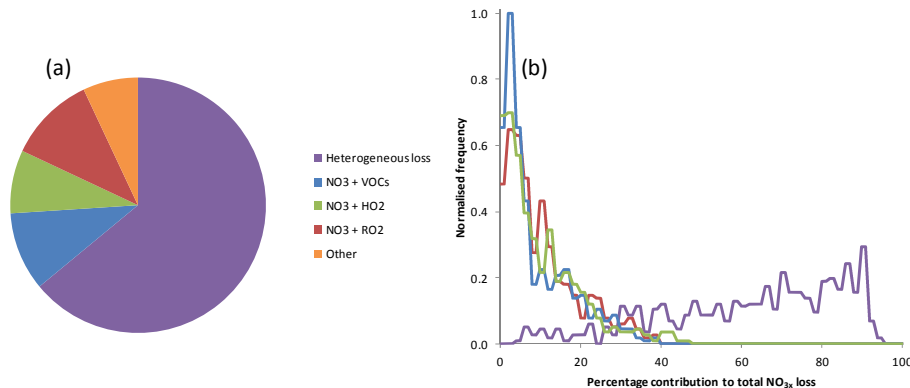


Fig. 3. Processes controlling losses of NO_{3x} ($= \text{NO}_3 + \text{N}_2\text{O}_5$) in the model, displayed as **(a)** the campaign mean and **(b)** the probability distribution functions for the percentage contributions to the total loss for heterogeneous uptake of NO_{3x} to aerosol surfaces (purple), $\text{NO}_3 + \text{VOCs}$ (blue), $\text{NO}_3 + \text{HO}_2$ (green) and $\text{NO}_3 + \text{RO}_2$ (all organic peroxy radicals) (red).

Radical chemistry at night

D. Stone et al.

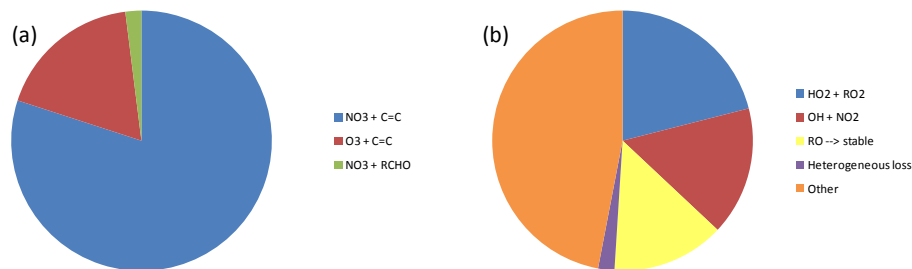


Fig. 4. Processes controlling the instantaneous production (a) and loss (b) of RO_x ($= RO + RO_2 + OH + HO_2$) radicals at night.

Title Page

Abstract

Introduction

Conclusions

References

Tables

Figures

◀

▶

◀

▶

Back

Close

Full Screen / Esc

Printer-friendly Version

Interactive Discussion



Radical chemistry at night

D. Stone et al.

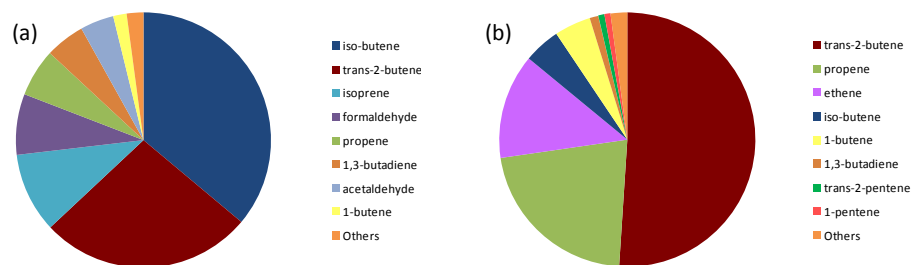


Fig. 5. Reactivity of (a) NO_3 and (b) O_3 towards observed volatile organic compounds (VOCs) at night during the RONOCO project.

Title Page

Abstract

Introduction

Conclusions

References

Tables

Figures

◀

▶

◀

▶

Back

Close

Full Screen / Esc

Printer-friendly Version

Interactive Discussion



Radical chemistry at night

D. Stone et al.

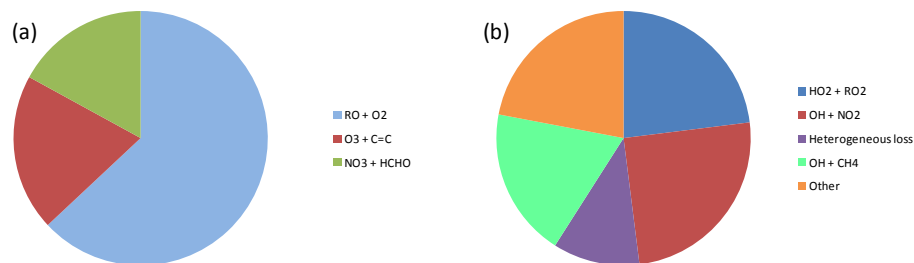


Fig. 6. Processes controlling the instantaneous production **(a)** and loss **(b)** of HO_x (= OH + HO₂) radicals at night.

[Title Page](#)[Abstract](#)[Introduction](#)[Conclusions](#)[References](#)[Tables](#)[Figures](#)[◀](#)[▶](#)[◀](#)[▶](#)[Back](#)[Close](#)[Full Screen / Esc](#)[Printer-friendly Version](#)[Interactive Discussion](#)

Radical chemistry at night

D. Stone et al.

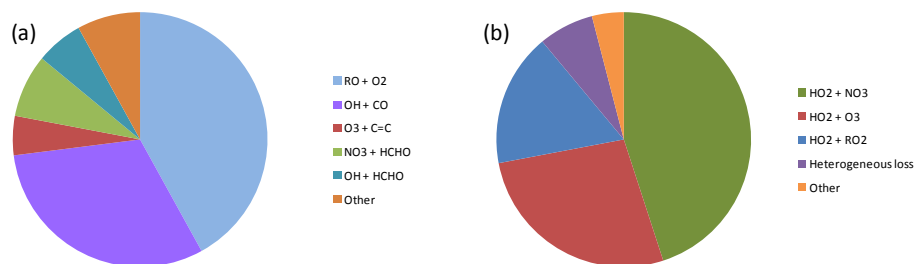


Fig. 7. Processes controlling the instantaneous production **(a)** and loss **(b)** of HO₂ radicals at night.

[Title Page](#)[Abstract](#)[Introduction](#)[Conclusions](#)[References](#)[Tables](#)[Figures](#)[I◀](#)[▶I](#)[◀](#)[▶](#)[Back](#)[Close](#)[Full Screen / Esc](#)[Printer-friendly Version](#)[Interactive Discussion](#)

Radical chemistry at night

D. Stone et al.

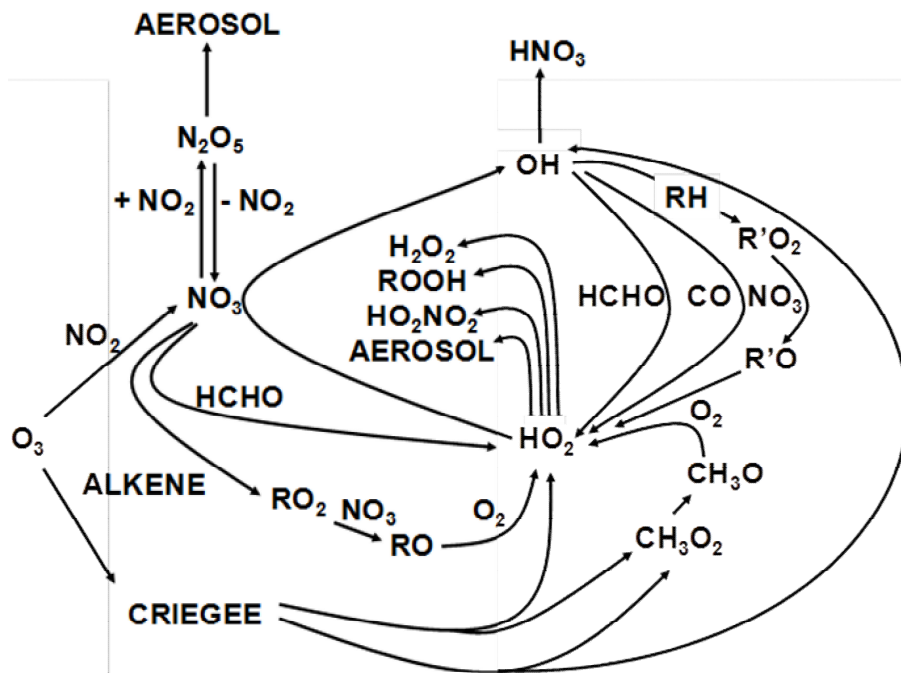


Fig. 8. Schematic summarising the dominant chemical pathways occurring during tropospheric oxidation at night during RONOCO.

Title Page	
Abstract	Introduction
Conclusions	References
Tables	Figures
◀	▶
◀	▶
Back	Close
Full Screen / Esc	
Printer-friendly Version	
Interactive Discussion	



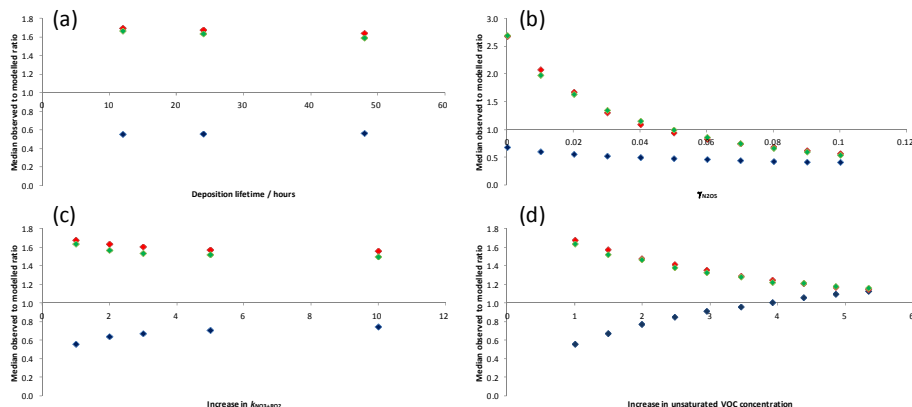


Fig. 9. Sensitivity of median modelled to observed ratios of HO_2^* (blue), NO_3 (red) and N_2O_5 (green) towards **(a)** the deposition lifetime adopted in the model; **(b)** $\gamma_{\text{N}_2\text{O}_5}$; **(c)** rate coefficients for $\text{NO}_3 + \text{RO}_2$ ($k_{\text{NO}_3+\text{RO}_2}$) adopted in the model; **(d)** concentrations of unsaturated VOCs in the model. Changes to $k_{\text{NO}_3+\text{RO}_2}$ and unsaturated VOC concentrations are represented as the factor by which $k_{\text{NO}_3+\text{RO}_2}$ and total unsaturated VOC concentration have been increased compared to the base run.

Title Page

Abstract

Introduction

Conclusions

References

Tables

Figures

◀

▶

◀

▶

Back

Close

Full Screen / Esc

Printer-friendly Version

Interactive Discussion



Radical chemistry at night

D. Stone et al.

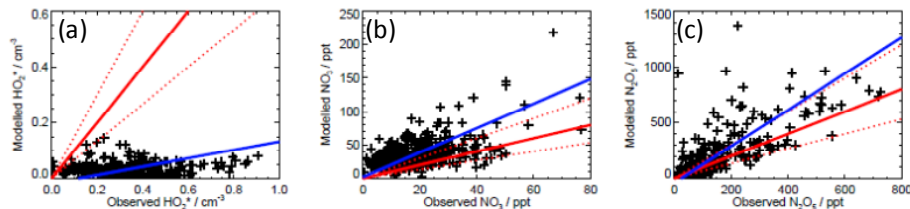


Fig. 10. Comparison between modelled and observed concentrations of **(a)** HO₂^{*}, **(b)** NO₃ and **(c)** N₂O₅ for a model run in which alkene concentrations are set to zero. In each plot, the solid red line indicates the 1 : 1 line, with 50% limits given by the broken red lines. The best fit lines are shown in blue, and are described by $[\text{HO}_2^*]_{\text{mod}} = \{(0.15 \pm 0.08) \times [\text{HO}_2^*]_{\text{obs}}\} - (1.75 \pm 2.55) \times 10^6 \text{ cm}^{-3}$ ($r^2 < 0.01$), $[\text{NO}_3]_{\text{mod}} = \{(1.83 \pm 0.18) \times [\text{NO}_3]_{\text{obs}}\} + (2.06 \pm 3.76) \text{ ppt}$ ($r^2 = 0.29$) and $[\text{N}_2\text{O}_5]_{\text{mod}} = \{(1.63 \pm 0.14) \times [\text{N}_2\text{O}_5]_{\text{obs}}\} - (39.20 \pm 22.19) \text{ ppt}$ ($r^2 = 0.61$).

Title Page

Abstract

Introduction

Conclusions

References

Tables

Figures

◀

▶

◀

▶

Back

Close

Full Screen / Esc

Printer-friendly Version

Interactive Discussion



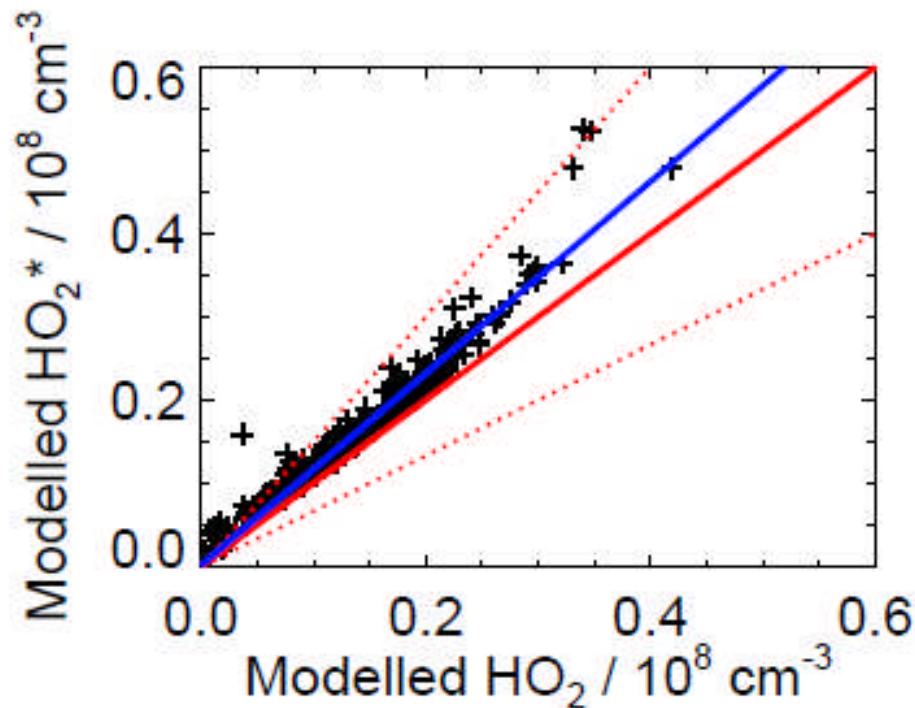


Fig. A1. Comparison between modelled HO_2^* (the sum of HO_2 and potential RO_2 interferences) and modelled HO_2 for RONOCO. The solid red line indicates the 1 : 1 line, with 50 % limits given by the broken red lines. The best fit line is shown in blue and is described by $\text{HO}_2^* = [1.15 \times \text{HO}_2] + 2 \times 10^5 \text{ cm}^{-3}$.

Radical chemistry at night

D. Stone et al.

Title Page	
Abstract	Introduction
Conclusions	References
Tables	Figures
◀	▶
◀	▶
Back	Close
Full Screen / Esc	
Printer-friendly Version	
Interactive Discussion	

